sustainability

MDPI

Article

Effective Deterministic Methodology for Enhanced Distribution Network Performance and Plug-in Electric Vehicles

Zeeshan Anjum Memon [1,2,3], Dalila Mat Said [1,2,*], Mohammad Yusri Hassan [1,2], Hafiz Mudassir Munir [4,*], Faisal Alsaif [5] and Sager Alsulamy [6]

1 Centre of Electrical Energy Systems (CEES), Institute of Future Energy (IFE), Universiti Teknologi Malaysia (UTM), Johor Bahru 81310, Johor, Malaysia
2 Faculty of Electrical Engineering, Universiti Teknologi Malaysia (UTM), Johor Bahru 81310, Johor, Malaysia
3 Department of Electrical Engineering, Mehran University of Engineering and Technology (MUET), SZAB, Campus, Khairpur Mirs 66020, Sindh, Pakistan
4 Department of Electrical Engineering, Sukkur IBA University, Sukkur 65200, Sindh, Pakistan
5 Department of Electrical Engineering, College of Engineering, King Saud University, Riyadh 11421, Saudi Arabia
6 Energy & Climate Change Division, Sustainable Energy Research Group, Faculty of Engineering & Physical Sciences, University of Southampton, Southampton SO16 7QF, UK
* Correspondence: dalila@utm.my (D.M.S.); mudassir.munir@iba-suk.edu.pk (H.M.M.); Tel.: +92-334-777-3939 (H.M.M.)

Abstract: The rapid depletion of fossil fuel motivates researchers and policymakers to switch from the internal combustion engine (ICE) to plug-in electric vehicles (PEVs). However, the electric power distribution networks are congested, which lowers the accommodation of PEVs and produces higher power losses. Therefore, the study proposes an effective deterministic methodology to maximize the accommodation of PEVs and percentage power loss reduction (%PLR) in radial distribution networks (RDNs). In the first stage, the PEVs are allocated to the best bus, which is chosen based on the loading capacity to power loss index (LCPLI), and the accommodation profile of PEVs is developed based on varying states of charge (SoC) and battery capacities (BCs). In the second stage, the power losses are minimized in PEV integrated networks with the allocation of DG units using a recently developed parallel-operated arithmetic optimization algorithm salp swarm algorithm (AOASSA). In the third stage, the charging and discharging ratios of PEVs are optimized analytically to minimize power losses after planning PEVs and DGs. The outcomes reveal that bus-2 is the most optimal bus for accommodation of PEVs, as it has the highest level of LCPLI, which is 9.81 in the 33-bus system and 28.24 in the 69-bus system. The optimal bus can safely accommodate the largest number of electric vehicles, with a capacity of 31,988 units in the 33-bus system and 92,519 units in the 69-bus system. Additionally, the parallel-operated AOASSA mechanism leads to a reduction in power losses of at least 0.09% and 0.25% compared with other algorithms that have been previously applied to the 33-bus and 69-bus systems, respectively. Moreover, with an optimal charging and discharging ratio of PEVs in the IEEE-33-bus radial distribution network (RDN), the %PLR further improved by 3.08%, 4.19%, and 2.29% in the presence of the optimal allocation of one, two and three DG units, respectively. In the IEEE-69-bus RDN, the %PLR further improved by 0.09%, 0.09%, and 0.08% with optimal charge and discharge ratios in the presence of one, two, and three DG units, respectively. The proposed study intends to help the local power distribution companies to maximize accommodation of PEV units and minimize power losses in RDNs.

Keywords: plug-in electric vehicle; power loss; AOASSA; loading capacity to power loss index (LCPLI)

Citation: Memon, Z.A.; Said, D.M.; Hassan, M.Y.; Munir, H.M.; Alsaif, F.; Alsulamy, S. Effective Deterministic Methodology for Enhanced Distribution Network Performance and Plug-in Electric Vehicles. *Sustainability* **2023**, *15*, 7078. https://doi.org/10.3390/su15097078

Academic Editor: Gaetano Zizzo

Received: 27 January 2023
Revised: 13 April 2023
Accepted: 19 April 2023
Published: 23 April 2023

1. Introduction

The rise in industrialization and community development predicts the consumption of electrical energy to rise by 50% in 2050 compared with 2018 [1]. The demand for

fossil fuels is also increasing due to the rise in power generation and road commutation. However, fossil fuels are limited in resources, and, recently, global oil prices also hiked due to the Russia–Ukraine invasion [2], requiring alternatives for power generation and road transportation. In the generation sector, a variety of work has been published on the smooth integration of solar and wind power generation with RDNs [3–6]. The market power pool players commercialize these two mature technologies around the globe. Alternatively, road transportation needs special attention since governments and policymakers encourage the use of plug-in electric vehicles (PEVs) for cleaner road commutation [7]. A recent survey indicates that 5 million PEVs were purchased in 2018, and the sales are predicted to elevate by 250 million in 2030 [8]. In addition, the transportation sector consumes a significant portion of total energy consumption among various sectors of electrical loads. The transportation load is expected to increase by 3.4% between 2013 and 2040, which is the highest compared with residential, commercial, and industrial loads [9]. The comprehensive literature indicates a rapid rise in the adoption and sales of PEVs [10,11]. Although the rise in PEVs is a remarkable indication of sustainable development, the shift from gasoline vehicles to energy-dependent PEVs poses severe challenges to the in-hand radial distribution networks (RDNs). In addition, the PEVs are stochastic, and the energy demand varies with the battery capacity (BC) and current state of charge (SoC). Since the conventional grids were not originally designed to accommodate the charging load of PEVs, only 10% integration of PEVs severely jeopardizes the performance of the distribution networks [12]. In addition, an increase in electric transportation increases power losses, resulting in higher financial losses to the local distribution companies [13]. The utility engineers and researchers propose two possible ways to accommodate the rising load of PEVs or minimize power losses in the PEV integrated networks. One of the promising solutions to deal with the issues is installing new generation units at the local level (which are termed distributed generators). Distributed generators (DGs) are small generating units placed close to the load centers and provide a variety of benefits to the grids [14–17]. Secondly, the PEVs also act as a great source of generating power and support the grid when required. It is estimated that PEVs are parked 95% of the day and the PEV batteries significantly reduce the power losses for local distribution companies [18].

1.1. Related Works

The comprehensive review of the literature indicates a variety of solutions for the smooth integration of PEVs. Zeng et.al [19] examined the effects of PEV charging on the hosting capacities of PEVs. The outcomes of the study indicate that the hosting capacity of selected nodes increases by 108% with the help of smart charging. However, the smart charging of PEVs is still at the pilot stage, since most power networks are not equipped with communication infrastructure [20]. Alternatively, installing DGs at the local level remains a viable solution to improve system performance in PEV integrated networks. Kongjeen et al. [21] optimized the size and locations of DGs at different levels of PEV injection to improve voltage, energy demand, and power losses with the aid of a genetic algorithm. The results indicate an improvement of 32.27%, 16.19%, and 44.70% in voltage, power losses, and demand, respectively. Khalid Mousa Hazazi [22] developed an optimal DG allocation-based methodology to minimize power losses and improve voltage profile in PEV integrated distribution networks. The outcomes of the study show that a power loss reduction of 76% and a voltage drop improvement of 4% were obtained. Fazelpour and Rosen [23] developed a DG allocation framework to reduce power losses in PEV integrated networks. The findings suggest that, by optimally sizing and placing distributed generation units, the reduction of power losses is 1.36%. The authors in [24] proposed a methodology to optimize the placement of photovoltaic charging stations to minimize voltage deviations, cost, and power losses in the IEEE-33-bus radial distribution network. The mentioned studies focused on minimizing power losses with optimal allocation of DG units; however, the capability to accommodate maximum PEVs is not assumed within the scope of the

mentioned studies. In actual practice, a system's capability to accommodate maximum PEVs is a prerequisite before the installation of DG units.

A variety of research studies address the problem of maximum accommodation of PEVs within the framework of DG allocation. Deng et al. [25] developed a mathematical model to maximize the accommodation of PEVs and minimize the cost. The participation of flexible resources elevates the accommodation of PEVs by 10%. [26] optimized the size and location of the energy storage system to maximize PEV penetration in the DC network using Monte Carlo simulations. The outcome of the study shows that 40 PEVs are safely accommodated considering the voltage constraint, while only 25 PEVs are accommodated considering current constraint violations. The study addresses DC networks only, while most in-hand distribution networks are AC in nature. Amini et al. [27] present an advanced methodology to minimize network losses and analyze PEV penetration against DG penetration. The research outcomes conclude that only a 5% increment in DG penetration increases PEV penetration by 25%. Shaaban et al. [28] present a detailed mathematical model for the energy consumption of PEV and later maximize PEVs with the optimal sizing and placement of DG units using GA. The results reveal that the optimal integration of distributed generation units increases the penetration of electric vehicles from 6 to 20%. Recently, a study [29] developed a methodology to maximize PEV accommodation and minimize power losses within the framework of DG allocation using PSO. The study suffers two methodological limitations. The study allocated the DG units first and then accommodated the maximum number of PEVs. However, the integration of PEVs is part of the planning stage and the PEVs should be allocated before the allocation of DG units. Furthermore, the DG sizes and locations are optimized using PSO, which is prone to local optima stagnation and results in higher power losses.

1.2. Research Contributions

From the comprehensive literature review, it is observed that the existing PEV and DG integrated studies suffer from three major limitations.

Firstly, the existing power distribution networks are not designed to accommodate PEVs because of their stochastic nature, which depends on numerous parameters (battery capacity, state of charge, etc.). Introducing PEVs in RDNs may congest the power lines and increase power losses. Thus, accommodating PEVs at the cost of increased losses or the converse is undesired as it deteriorates the network performance. It necessitates the adoption of a compromised strategy to attain an optimum solution. The existing studies maximized the accommodation of PEVs [19,25,26,28,30–35] while others reduced network power losses [21–23,27,29,36–41]. Thus, the combined handling of both objectives within a single framework has been ignored, which is not a practical approach. The detailed analysis reveals that only one recent study [29] focuses on PEV maximization and power loss minimization. However, the study suffers from limitations in methodology. The methodology suffers from limitations in the way the PEVs and DGs are allocated, and the optimization technique used for the allocation of DG units suffers from inherent limitations in the search mechanism. The study allocated the DG units first, then allocated PEVs, which is not a practical approach. Practically, PEV units are allocated first, then DG units are allocated based on maximum loading of PEVs.

Secondly, from the available literature, it is observed that the optimization problems in PEV integrated networks are solved with analytical algorithms [19,26,30,32,34,35,38], metaheuristic algorithms [21,23,25,27,28,31,33,36,37,39–41] and hybrid metaheuristic algorithms [22]. It is also observed that the optimal power flow method or Monte Carlo simulations are among the analytical methods used in the literature. Among the metaheuristic algorithms, the genetic algorithm (GA), particle swarm optimization (PSO), and differential evolution (DE) are widely used. Among the hybrid algorithms, simulated annealing particle swarm optimization (SAPSO) is used. Contrarily, the literature also states that the analytical algorithms are less complex and have a fast execution time. However, while solving the DG allocation problem, neither simplicity nor convergence speed is of

utmost importance. Since DG allocation is a planning problem, convergence speed is not a significant factor. The simulation time can take hours to find the optimal solution as long as good accuracy is obtained. The planning studies focus on the accuracy of algorithms to choose optimal decision variables, whereas the analytical methods are observed to lack accuracy in complex combinatorial optimization problem. Although metaheuristic algorithms are more intelligent than analytical methods, they have some limitations. For instance, GA is an intelligent algorithm to search for global solutions but suffers from parameter tuning issues, complicated mutations, and cross-over operators. PSO is a competent algorithm but suffer from local optima stagnation. Generally, the metaheuristic algorithms are inferior to hybrid algorithms, since the former algorithms suffer from inherent deficiencies. Among different types of algorithms, hybrid techniques are considered more accurate and efficient than individual algorithms since they combine the searching capabilities of two different methods. In contemporary literature, the hybridization of different techniques has been dealt with using a sequential approach, where optimal solutions produced by one algorithm are fed as an input to another. Thus, the former algorithm guides the search direction of the latter. It is known that all optimization algorithms suffer from some inherent deficiencies. Therefore, if the first algorithm's solutions are stuck in the local optimum, the latter's solutions are also drawn to approach this local optimum; hence, population diversity is lost. For this reason, it is imperative to propose an effective method that overcomes the highlighted deficiency of the sequential hybridization approach. In addition, there are no set guidelines for choosing two techniques for hybridization; however, the main goal behind combining two approaches is that they must aid each other in overcoming their weaknesses. The need to combine one technique with another usually arises to enhance their exploration and exploitation abilities or maintain population diversity. The arithmetic optimization algorithm (AOA) and salp swarm algorithm (SSA) are two recently introduced effective metaheuristic techniques in the literature. However, the followers in the salp swarm algorithm produce a relatively higher diversity of particles in the exploitation phase, and, consequently, the algorithm is not capable of converging to an optimal solution. As a result, the SSA suffers from inherent exploitation capabilities. On the other hand, the AOA's updation mechanism illustrates that the obtained solutions concentrate primarily on searching for the best solution. It minimizes the population diversity during the exploration phase and increases the likelihood of premature convergence and local optima stagnation. These inherent limitations of SSA and AOA can lead to suboptimal DG unit allocation and increased power losses in RDNs. Therefore, it is essential to propose a suitable hybridization mechanism for AOA and SSA that enables them to overcome their limitations and attain an improved optimal solution.

Thirdly, once the PEVs and DGs are allocated, it is not convenient or feasible to reallocate them. Under such circumstances, V2G plays a significant role in minimizing active power losses, Although a variety of studies have focused on power loss minimization with V2G [22,23,37]. The coordination of charging and discharging minimizes the detrimental impact of PEVs on the grid and helps to increase the system's efficiency in various ways. However, neither discharging 100% PEVs (i.e., V2G) nor charging 0% PEVs (i.e., G2V) results in minimum power losses. By managing the optimal share of charging and discharging PEVs, it is possible to prevent the overload of distribution lines, and improvement in the efficiency of distribution networks can be gained. Although the presented studies in the literature have minimized power losses with V2G, the selection of optimal PEVs' charging–discharging ratios has been ignored.

In the light of highlighted limitations, the proposed study has four contributions, which are highlighted as:

- Development of a deterministic methodology for maximizing the accommodation of PEVs and minimizing power losses in IEEE-33-bus and IEEE-69-bus radial distribution networks;
- Development of a methodology for optimal sizing and location of distributed generation (DG) units with the parallel-operated arithmetic optimization algorithm salp

swam algorithm (AOASSA) for minimizing active power losses in PEV integrated IEEE-33-bus and IEEE-69-bus radial distribution networks;
- Development of charging and discharging profiles of PEVs and analysis of optimal charge and discharge ratios of PEVs for achieving the least power losses with different numbers of allocated DG units;
- Comparative analysis of the parallel-operated hybrid arithmetic optimization algorithm salp swam algorithm (AOASSA) against the standard arithmetic optimization algorithm (AOA), the salp swarm optimization algorithm (SSA), the particle swarm optimization algorithm (PSO), and hybrid salp swarm optimization algorithm particle swarm optimization (SSAPSO) on IEEE-33 bus and IEEE-69 bus radial distribution networks (RDNs).

The rest of the paper is arranged as follows. Section 2 comprises research methodology. Section 3 comprises results and discussions. Lastly, Section 4 comprises conclusions and future works.

2. Research Methodology

The research design and procedure presented in this section aims to enhance the integration of electric vehicles while minimizing power losses. The proposed methodological framework is classified into three main stages, which include the maximization of PEVs on the best bus location based on LCPLI, minimization of power losses in the PEV integrated network using the proposed AOASSA algorithm, and optimization of PEV charge and discharge ratios for power loss minimization. The proposed methodological framework is presented in Figure 1. The methodology is individually elaborated in Sections 2.1–2.3.

2.1. Stage 1 Maximization of PEV Accommodation on the Best Bus

This section presents the methodology to maximize the accommodation of PEVs and evaluate the maximum number of PEVs accommodated on the best bus at different SoC and BCs. The proposed study presents an analytical technique to accommodate the maximum number of PEVs in RDNs. Initially, all the buses are kept at standard loadings. The base case power flow is executed, and the power losses are observed. Let *i* be the current bus location and K be the maximum number of buses. Initially, the bus index (i) is set to 2 (since the first bus is a slack bus) and is compared against K. The load on the *i*th bus is increased from the standard loading point to the point where the power system constraints violate (symbolized as l_{max}) and is expressed by Equation (1).

$$l_{max} = l_{stnd} + dl_{c.o} \tag{1}$$

where l_{stnd} is the standard loading on *i*th bus and $dl_{c.o}$ is the increase in original loading at which the network constraints violate.

The maximum loading point (l_{max}) is observed, and the power flow is executed. The power losses (P_{loss}) are calculated using Equation (2).

$$P_{loss} = I^2R \tag{2}$$

(l_{max}) and P_{loss} are stored in the memory of the variable. The process of evaluating l_{max} and P_{loss} continues for all buses in RDNs. After computing l_{max} and P_{loss} in RDNs, the loading capability to power loss index (*LCPLI*) is computed for all buses to accommodate PEVs. The *LCPLI* is expressed in Equation (3).

$$LCPLI = \frac{l_{max}}{p_{loss}} \tag{3}$$

where l_{max} represents maximum loading and P_{loss} represents power losses on the *i*th bus location at the maximum loading point. The *LCPLI* is computed for the K buses.

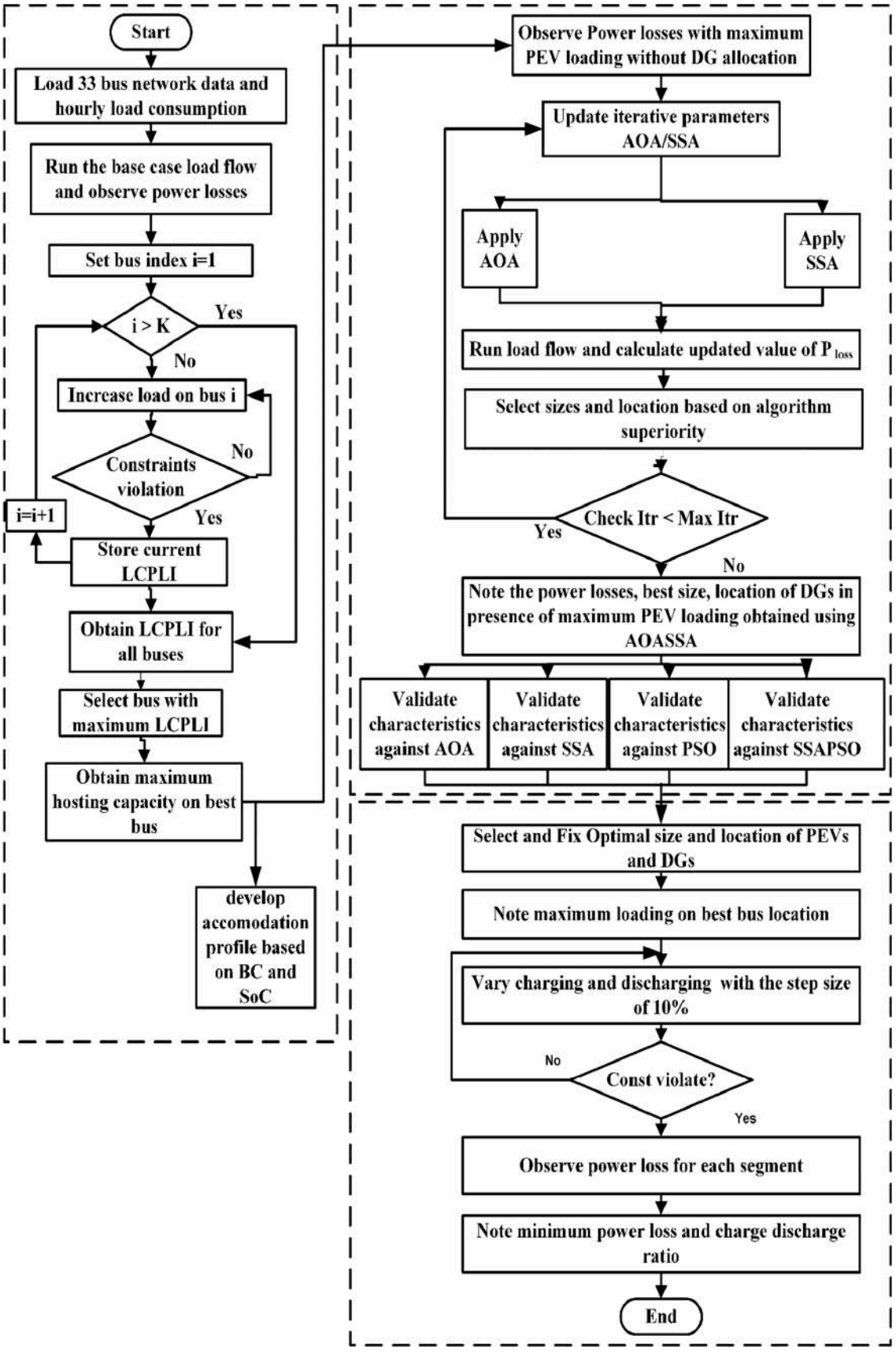

Figure 1. Proposed methodological framework.

The bus with the highest $LCPLI$ is the best bus to accommodate PEVs in the network. After deciding the best bus to accommodate PEVs, the amount of energy available for PEVs is calculated. The additional energy available for PEVs ($E_{available}$) is calculated using Equation (4) and is expressed as follows

$$E_{available} = dP_{i,BEST} \times t \tag{4}$$

where $dP_{i,BEST}$ is the power consumed by the load $dl_{c.o}$ in time t hours at the best bus location. The number of PEVs accommodated at any time t depends on the energy available at that time ($E_{available,t}$) and the energy consumed by PEVs. The number of PEVs ($N_{pev,t}$) accommodated in the t^{th} hour is expressed in Equation (5)

$$N_{pev,t} = \frac{E_{available,t}}{E_{PEV,t}} \tag{5}$$

where $E_{PEV,t}$ is the energy consumption of the Pth PEV. The energy consumption of the Pth PEV is highly dependent on the state of charge (SoC) and battery capacity (BC). The $E_{PEV,t}$ is the energy consumed by the Pth PEV and is calculated with the help of Equation (6), which is expressed as follows.

$$E_{pev,t} = E^t_{pev,soc} - E^t_{pev,initialsoc} \tag{6}$$

where $E^t_{pev,initialsoc}$ is the energy stored in the PEV battery at initial conditions (before charging) and $E^t_{pev,soc}$ is the energy consumed by the Pth PEV at any time t, which is expressed with the aid of Equation (7).

$$E^t_{pev,soc} = 0.8 \times E_{max}\left(1 - e^{\frac{-\alpha \times t_{req}}{t_{max}}}\right) + E_0 \tag{7}$$

The time required (t_{req}) to charge the Pth electric vehicle battery from its initial state of charge (E_0) to its final state of charge (80%) by using a level 2 charger for a maximum time of five hours is presented in Equation (8). The charging time is calculated by multiplying by a factor of 0.8, which represents the recommended 80% maximum energy from the battery by the manufacturers, and the time constant is represented by α.

$$t_{req} = \begin{cases} 0; if\ E_0 = E_{max} \\ t_{max}; if\ E_0 = 0 \\ \frac{-t_{max}}{\alpha} ln \frac{E_0}{E_{max}}; if\ 0 < E_0 < E_{max} \end{cases} \tag{8}$$

where E_{max} is the battery capacity (kWh) and its value is specified by the manufacturer, α is a charging constant and its value is 8.4428, t_{max} is the time required to charge a battery from 0 to 100% SoC, which is 5 h for a considered level 2 charger (7.2 kW), and E_0 is the initial energy stored in the PEV battery (at the initial state of charge). The flow chart of the proposed mechanism to maximize PEV on the best bus and obtain the accommodation profile at different BCs and SoC of PEVs is depicted in Figure 2.

2.2. Power Loss Minimization with Optimal Allocation of Distributed Generation

In this section, a methodology for minimizing power losses in networks integrated with a maximum loading of electric vehicles is proposed, which is based on the optimal allocation of distributed generation units. Initially, problem formulation and network constraints are discussed in Sections 2.2.1 and 2.2.2, respectively. Then the methodology for a hybrid AOASSA is presented in Section 2.2.3.

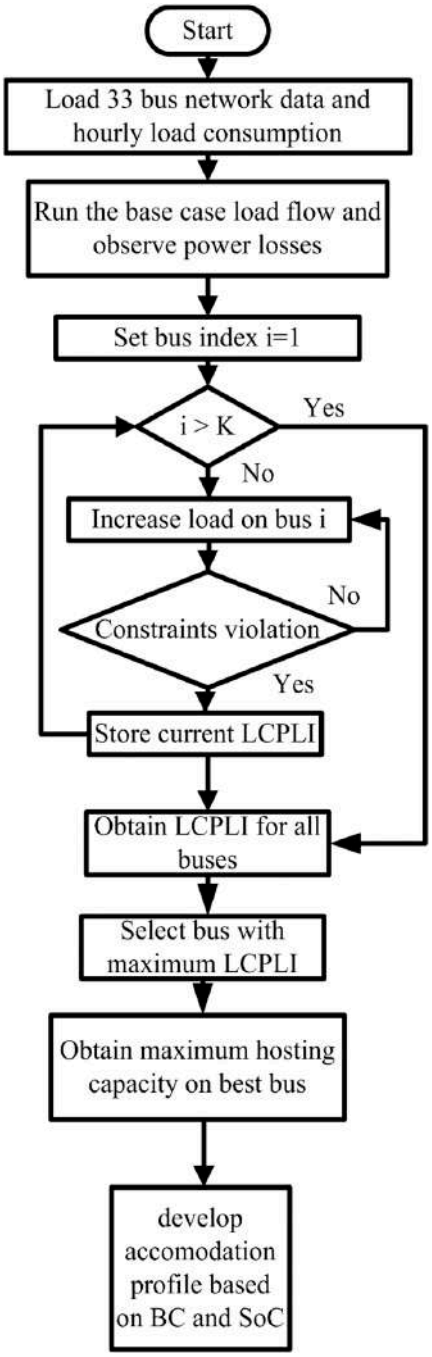

Figure 2. Mechanism to maximize PEV on best bus and obtain the accommodation profile.

2.2.1. Problem Formulation

Active power losses are more prevalent than reactive power losses in distribution networks. In distribution networks, the distances are relatively shorter, which results in more active power losses compared with the transmission networks. Additionally, the distribution network typically has more branches and connections than the transmission network, which also contributes to the higher active power losses. The objective function of the proposed study is to minimize active power losses when the system is integrated with maximum PEV loading. The objective function is generally stated in Equation (9).

$$ObjectiveFunction = Minimize(P_{loss}) = Minimize\sum_{i=1}^{N} I_i^2 R_i \quad (9)$$

where I_i indicates the current flow through the ith branch, R_i indicates the resistance of the ith branch, and N is the total number of branches. The power loss function indicates that the power losses depend on the current flow in the branches, which depend on the sizes and locations of the DG units in the network.

Therefore, optimizing the DG capacity and placement for power loss minimization is crucial. The percentage power loss reduction (%PLR) is mathematically expressed with the aid of Equation (10).

$$\%\ PLR = \frac{P_{loss(without\ DG)} - P_{loss(with\ DG)}}{P_{loss(without\ DG)}} \times 100 \quad (10)$$

Equation (10) compares the power losses in the network without and with the allocation of distributed generation units, where $P_{loss(withoutDG)}$ refers to the power losses without DG and $P_{loss(withDG)}$ refers to the power losses with DG allocation.

2.2.2. Network Constraints

This section presents the set of constraints considered for power loss minimization. Constraints are the conditions that must not be exceeded while attempting to achieve the goal of the optimization problem, whether it is to minimize or maximize the objective function. In power distribution networks, the power losses are desired to be minimum while the voltages active and reactive power supply are within set limits. The considered network constraints are presented with the aid of Equations (11) to (14).

$$\sum_{j=1}^{Nbus} P_{load}^{j} + \sum_{i=1}^{N\ branches} P_{loss}^{i} > \sum_{i=1}^{Z\ DGs} P_{DG}^{Z} \quad (11)$$

$$\sum_{i=1}^{Nbus} Q_{load}^{j} + \sum_{i=1}^{N\ branches} Q_{loss}^{i} > \sum_{i=1}^{Z\ DGs} Q_{DG}^{Z} \quad (12)$$

$$0.90\ \text{p.u} < V_J > 1.05\text{p.u} \quad (13)$$

$$\mathrm{I_{phase}} < 300\text{A} \quad (14)$$

where the P_{load}^{j} indicates the active load, Q_{load}^{j} indicates the reactive load on the jth bus, P_{DG}^{Z} represents the active power delivered by zth DG, Q_{load}^{j} represents the reactive load by zth DG, V_J indicates the voltages on jth bus, and $\mathrm{I_{phase}}$ represents the phase current.

2.2.3. Parallel Operated Hybrid Arithmetic Optimization Algorithm Salp Swarm Algorithm

The parallel-operated hybrid AOASSA algorithm is an efficient algorithm that improves the search capability for the optimal placement and size of distributed generation units in networks integrated with electric vehicles. The hybrid AOASSA algorithm mitigates the inherent deficiencies in standard AOA and SSA. Furthermore, the parallel-operated mechanism indicates that each algorithm runs independently, and no algorithm feeds other algorithms. This section presents the step-by-step methodology for power loss minimization using a parallel-operated hybrid AOASSA algorithm. The methodology for the parallel-operated hybrid AOASSA algorithm to optimize size and location of DG units is presented in Figure 3 and the step-by-step methodology is presented underneath.

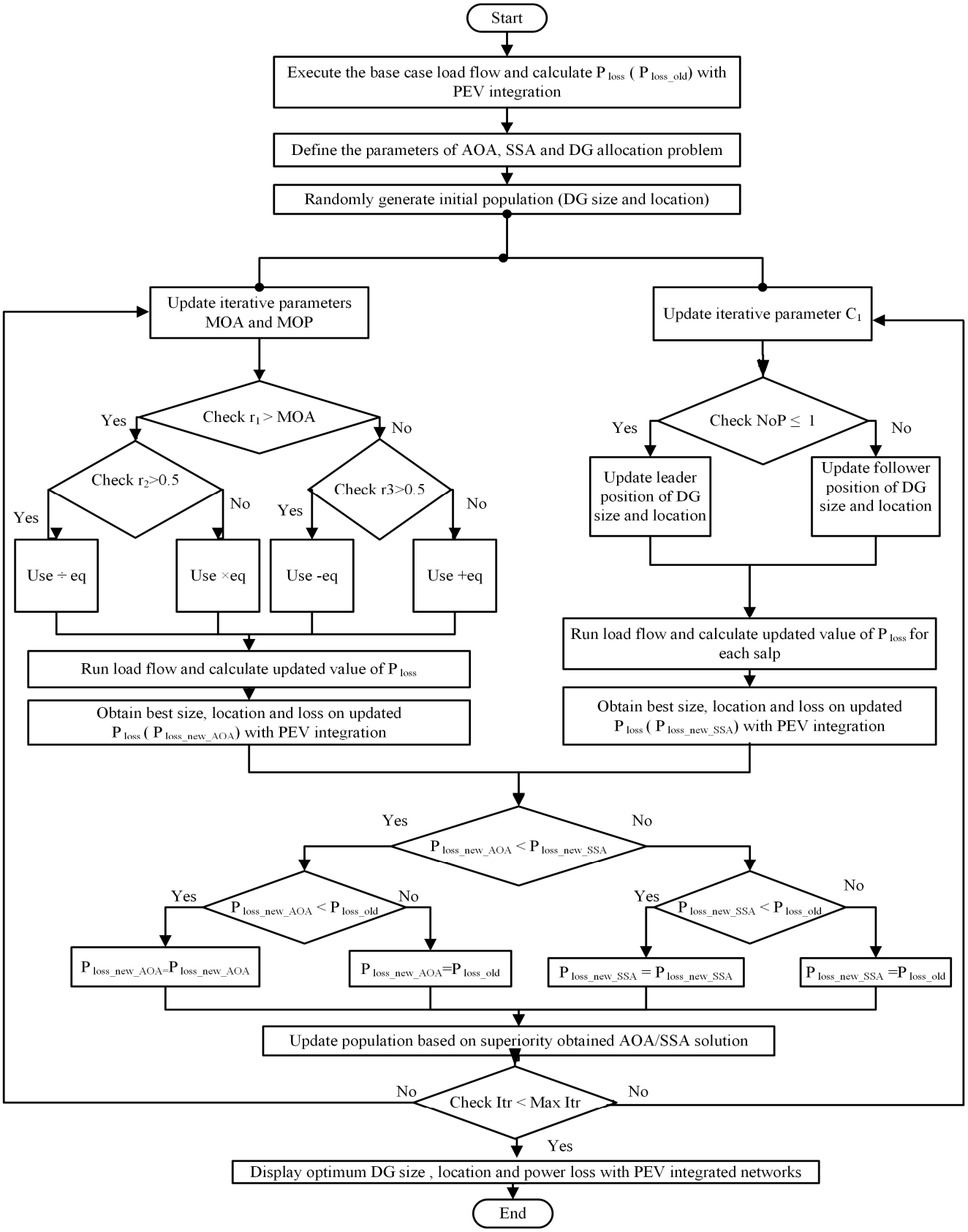

Figure 3. Flow chart of the proposed parallel-operated AOASSA for DG allocation in PEV integrated networks.

Step 1: Define the load and line data of 33-bus RDN [42].

Step 2: Run the load flow and evaluate power losses (Ploss_old) without allocation of DG units.

Step 3: Specify the parameters for optimal sizing, sitting of DGs, and optimization algorithms, i.e., AOA and SSA [43].

Step 4: Initialize the placements and capacities of the DG units randomly. The set of potential solutions for Z DGs be x and the set of decision variables (sizes and locations) represented by y are presented in Equation (15).

$$Z = \left[\begin{array}{ccc||ccc} P_{DG1,1} & P_{DG1,2\ldots\ldots} & P_{DG1,y} & N_{DG1,1} & N_{DG1,2\ldots\ldots} & N_{DG1,y} \\ P_{DG2,1} & P_{DG2,2\ldots\ldots} & P_{DG2,y} & N_{DG2,1} & N_{DG2,2\ldots\ldots} & N_{DG2,y} \\ \vdots & \vdots & \vdots & \vdots & \vdots & \vdots \\ \vdots & \vdots & \vdots & \vdots & \vdots & \vdots \\ \vdots & \vdots & \vdots & \vdots & \vdots & \vdots \\ P_{DGx,1} & P_{DGx,2} & P_{DGx,y} & N_{DGx,1} & N_{DGx,2\ldots\ldots} & N_{DGx,y} \end{array}\right] \quad (15)$$

Step 5: Use Equations (16) and (17) to update MOA and MOP, respectively, and run load flow using AOA [44].

$$MOA\ (C\_iter) = Min + C\_iter\frac{Max - Min}{M\_iter} \quad (16)$$

$$MOP(C\_iter) = 1 - \frac{C\_iter^{\frac{1}{\alpha}}}{M\_iter^{\frac{1}{\alpha}}} \quad (17)$$

where MOA(C_iter) denotes the math operator accelerated for tth iteration, and C_iter represents the current iteration, which is in between 1 and the maximum number of iterations. Max and Min represent the maximum and minimum values of an accelerated function, MOP(C_iter) represents the math operator probability for the current iteration, α represents the sensitivity parameter, and M_ITER stands for the maximum number of iterations that the algorithm will perform.

Step 6: Check the value of the randomly initiated parameter r_1. If the value of r_1 is greater than MOA for current iteration, then compare the value of r_1 with r_2. If the randomly initiated parameter r_2 is greater than 0.5, then use the division equation (Equation (18), first part) to update the capacity and placement of DG units. In either case, if r_2 is less than 0.5, use the multiplication equation (Equation (18), 2nd part) to update the placement and capacity of DG units. The function MOA increases after number of iterations and MOA exceeds the randomly initiated parameter r_1, then compare r_1 with r_3. If r_3 is greater than 0.5, use the subtraction equation (Equation (19), first part) to update DG size and location. In either case, if r_3 is less than 0.5, use the addition equation (Equation (19), 2nd part) to update DG size and location.

Where $X_{i,j}(\mathrm{C_{iter}} + 1)$ indicates the solution in the upcoming iteration, $Bestx_j$ indicates the best obtained position in the jth place, Ub_j and Lb_j indicate the upper and lower bounds, respectively, r_2 represents a randomly generated integer that balances exploration and exploitation, $\in$ is an integer value (very small), and μ is the control parameter.

$$X_{i,j}(\mathrm{C_{iter}} + 1) = \begin{cases} Bestx_j \div \left((MOP + \in) \times \left(Ub_j - Lb_j\right) \times \mu Lb_j\right) & r_2 < 0.5 \\ Bestx_j \times \left((MOP + \in) \times \left(Ub_j - Lb_j\right) \times \mu Lb_j\right) & otherwise \end{cases} \quad (18)$$

$$X_{i,j}(\mathrm{C_{iter}} + 1) = \begin{cases} Bestx_j - \left((MOP + \in) \times \left(Ub_j - Lb_j\right) \times \mu Lb_j\right) & r_3 > 0.5 \\ Bestx_j + \left((MOP + \in) \times \left(Ub_j - Lb_j\right) \times \mu Lb_j\right) & otherwise \end{cases} \quad (19)$$

Step 7: Evaluate the updated active power loss value (P_{loss}) using Equation (2).

Step 8: Obtain the power loss value updated (abbreviated as Ploss_new_AOA) and respective size/sizes/location/locations of DG units by AOA.

Step 9: Apply SSA, and initially update the value of c_1 with the aid of Equation (20), which is presented as

$$c_1 = 2e^{-\left(\frac{4l}{L}\right)^2} \tag{20}$$

where the notation l indicates the number of current iterations, and the notation L indicates the number of maximum iterations. The parameter c_1 is helpful to maintain the exploration and exploitation.

Step 10: Check the population count (NoP); if the NoP is 1, then update the leader position with the aid of Equation (21), and in the either case use Equation (22) to update the follower position [44].

$$x_i^1 = \begin{cases} y_i + c_1\left((Ub_i - Lb_i) \times c_2 + Lb_i\right) & c_3 \geq 0.5 \\ y_i - c_1\left((Ub_i - Lb_i) \times c_2 + Lb_i\right) & c_3 < 0.5 \end{cases} \tag{21}$$

$$x_i^j = \frac{(x_i^j + x_i^{(j-1)})}{2} \tag{22}$$

where x_i^1 indicates the position of the first salp in the ith dimension, y_i indicates the food position in the ith dimension, and the parameters Lb_i and Ub_i indicate the lower and upper bounds, respectively. The coefficients c_2 and c_3 are randomly initiated numbers lying between 0 and 1.

Step 11: Obtain the power losses from individual salps and run the load flow analysis.

Step 12: Obtain the best DG size and location (termed as Ploss_new_SSA).

Step 13: Compare power losses obtained with AOA and SSA (step 8 and step 12); if the power loss obtained with AOA is less than the value of power loss obtained with SSA, then compare the value of power loss obtained with AOA with the initial power loss value, then update the value of power loss with power loss value obtained with AOA. In either case, the initial value of power loss holds the same value (updated). Alternatively, if the power loss value obtained with SSA is smaller than that obtained with AOA, update the value of power loss with the power loss value obtained with SSA. Furthermore, check if the value of power loss obtained with SSA is smaller than initial power loss value, and update the value of power loss obtained with SSA.

Step 14: Update the value of DG size and location with the superior solution. The superiority of the solution is based on the value of power losses.

Step 15: Repeat the program up to the maximum preset value of iterations (200 iterations).

2.3. Stage 3 Optimal Charge and Discharge Ratios for Power Loss Minimization

This section presents the methodology for optimal charge and discharge ratios to minimize power loss. The DGs and PEVs are allocated at the planning stage and the utility lacks the authority to change the position or sizes of DGs, once allocated. The DGs can neither be re-sized nor re-located immediately from one location to another in the operational phase. The PEVs are also fixed at the best bus location. The optimal charge and discharge ratios are a promising option to minimize the power losses in pre-allocated PEVs and DGs. Therefore, the methodology is presented to optimize the charge and discharge ratios of PEVs and minimize the power losses in the RDN.

Proposed Methodology for Optimal Charging and Discharging of PEVs

This section presents the methodology to optimize the charge and discharge ratios of the PEVs for power loss minimization in pre-allocated PEVs and DG networks. The charging of PEVs is considered as the load and discharging of PEVs is considered the source of power generation. The load is opposite to the generation; therefore, the proposed study considers load as negative of generation and vice versa. The standard loading of the bus is kept constant.

The charging and discharging of PEVs on the best bus location vary the power injections into the distribution system. The variation in power injections varies the power losses in the network. The proposed study presents a methodology to find the optimal power injections by varying charge and discharge ratios for power loss minimization. The maximum loading capacity of the best bus is allocated to PEVs and is segmented into ten equal ratios, as shown in Figure 4. Let l_{max} be the maximum loading at which the power system constraints violate, then the maximum loading capability available for PEV loading is expressed with the help of Equation (23).

$$dl_{c.o} = l_{max} - l_{stnd} \tag{23}$$

where $dl_{c.o}$ represents the maximum loading capability available for PEVs loading and the vector of $dl_{c.o}$ is segmented into ten equal segments (in other word; cases). The segmentation of vector $(dl_{c.o})$ is expressed with the help of Equation (24) and is presented as.

$$dl_{c.o} = [dl_{c.o,1}, dl_{c.o,2} \ldots\ldots\ldots\ldots\ldots\ldots\ldots dl_{c.o,10}] \tag{24}$$

where $dl_{c.o,1}$ represents the first segment of the dedicated PEV loading and $dl_{c.o,10}$ represents the tenth segment of the total loading (equal to the maximum allowable loading for PEVs). In the proposed methodology, segment $dl_{c.o,1}$ represents 10% of the $dl_{c.o,10}$ and it reflects that 10% PEVs are discharging while the remaining 90% PEVs are charging from the selected bus location. The power injections $(P_{injection})$ are determined for all the segments and the power losses are determined by using load flow analysis. Therefore, the total power injection from the best bus location is expressed with the help of Equation (25).

$$P_{injection} = P_{injection,PEV\_discharging} - P_{injection,PEV_{charging}} - l_{stnd} \tag{25}$$

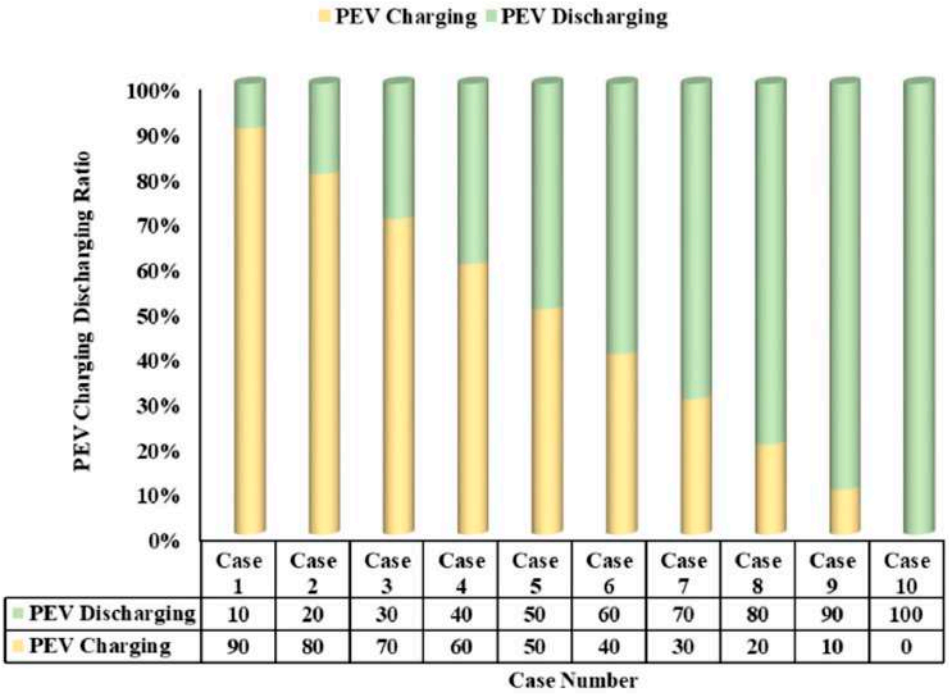

	Case 1	Case 2	Case 3	Case 4	Case 5	Case 6	Case 7	Case 8	Case 9	Case 10
PEV Discharging	10	20	30	40	50	60	70	80	90	100
PEV Charging	90	80	70	60	50	40	30	20	10	0

Figure 4. Scenarios of charge and discharge ratios of PEVs.

The power injection on the best bus depends on PEV charging and discharging ratios. Therefore, varying the charging and discharging of PEVs varies the power injection at the best bus and ultimately changes power losses. The methodology is repeated for the remaining segments on the best bus by varying ratios of charging and discharging of PEVs.

The methodology for the optimal charge and discharge ratios is presented in Figure 5. Initially, the best bus is selected based on LCPLI (obtained at the end of the first stage). The maximum loading available for PEVs is noted and is divided into segments. Each segment represents a 10% variation in charging and discharging ratios. The segments are increased and are compared with total allowable loadings. If the increased load does not exceed the total allowable loading, the program increases the load segments and stores the value of power loss. However, if the incremental load exceeds the total allowable loading capacity dedicated for PEVs, the program terminates and the power losses and respective charge–discharge ratios are stored. The charge and discharge ratios with minimum power loss are the optimal charge and discharge ratios.

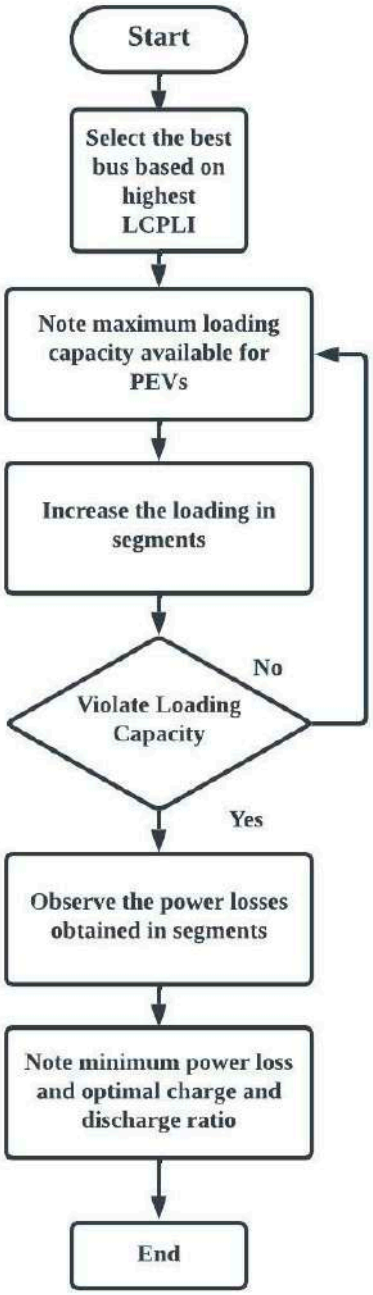

Figure 5. Methodology for optimal charge and discharge ratios.

3. Results and Discussions

The research procedure of the proposed study is divided into three main stages. The outcomes of the first stage are utilized as input to the second stage, and the outcomes of the second stage are used as input to the third stage. The detailed methodology of the three stages is presented in Section 2. In this section, the outcome of each stage is presented. The proposed research methodology is implemented on IEEE-33-bus radial distribution networks (RDNs) to investigate and validate the effectiveness of the proposed methodology. The backward/forward load flow is run to retrieve the values of bus voltages, line currents, and power flows. The backward/forward theorem provides an efficient, robust, and effective mechanism for analyzing RDNs. In the first stage, the optimal location and capacity are determined using the analytical method to maximize the accommodation of PEVs in the RDN. The optimal location and capacity to maximize PEVs in the RDN is based on the LCPLI. The bus with the highest LCPLI is chosen as best bus to accommodate PEVs. The accommodation profile is shown at different battery capacities and state of charge (SoC). In the second stage, the sizes and locations of the DG units are optimized to minimize active power losses in PEV integrated networks. The study proposes an AOASSA-based methodology to optimize the sizes and locations of DG units in PEV integrated networks. The power losses, convergence characteristics, and robustness (statistical analysis) obtained by AOASSA are compared with the standard AOA, SSA, PSO, and hybrid SSAPSO. It is assumed that the DGs supply active power and only active power losses are minimized in test network. In the third stage, an additional feature of V2G is introduced in cases of pre-allocated PEVs and DGs. The allocation of PEVs and DGs on best bus are fixed; neither the sizes nor location of PEVs can be changed, and neither the sizes nor locations of DGs can be changed. In such a case, the V2G mechanism is introduced to minimize the active power losses in the operation phase. The charging and discharging ratios are optimized to minimize active power losses. The discharging of 100% PEVs and charging of 0% PEVs neither guarantee minimum power losses nor are a practical case in real-time RDNs. Therefore, charging and discharging ratios of PEVs are optimized to minimize active power losses in RDNs. The methodology is implemented on a 33-bus radial distribution network (RDN). The standard active and reactive loadings of IEEE 33-bus RDN are 3.715 MW and 2.3 MVARs, respectively. Node 1 receives 12.66 kV through a step-down transformer. The standard power loss (without loading of PEVs or DGs) is 211 kW. The topology of a 33-bus RDN is presented in Figure 6a. The typical 69-bus RDN, on the other hand, has a balanced load arrangement with an active load of 3.80 MW and a reactive load of 2.69 MVAr. The voltage is reduced to 12.66 kV before node 1 by a step-down transformer. A 69-bus has real power losses of 225 kW. A typical topological structure of both the buses is presented in Figure 6a,b.

3.1. Selection of Best Bus for Accommodating PEVs

Initially, the proper allocation of PEVs is planned. The PEVs are allocated based on the LCPLI. The buses in the 33-bus RDN are subjected to the variations in loading and the LCPLI for individual buses is calculated. The load on an individual bus varies with the step size of 0.01 MW, and the distribution network constraints are checked. The bus with the highest loading capability to power losses indicates that the bus can handle higher loading with the least power losses. The bus holding the highest value of LCPLI is the best bus to accommodate PEVs. The simulations indicate that the bus-2, bus-19 and bus-20 hold the highest value of the LCPLI. Among, the top three buses, bus-2 holds the highest value of the LCPLI (which is 9.81 units) and is considered the best bus to accommodate PEVs. The LCPLI for the 33-bus RDN is presented in Table 1.

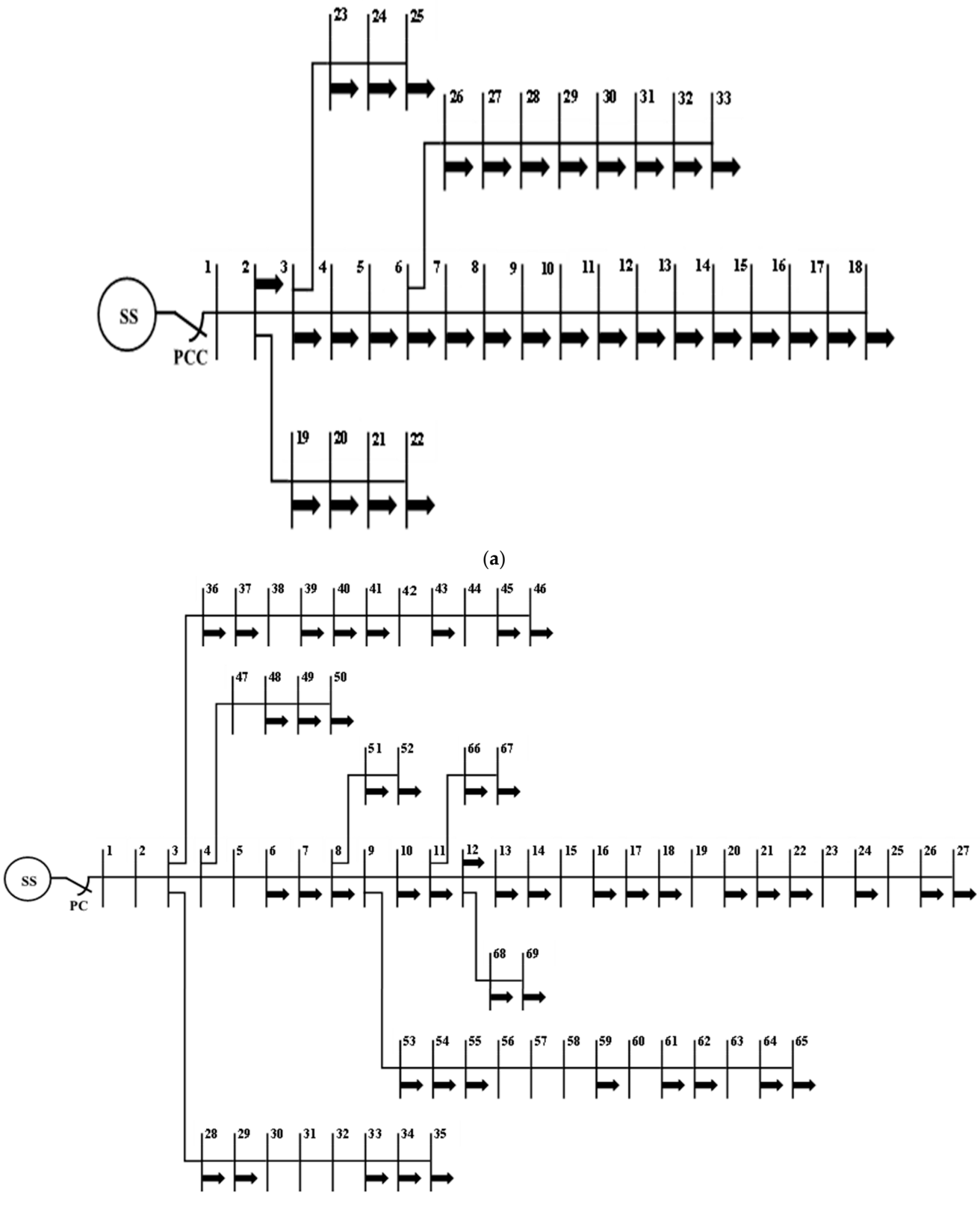

Figure 6. (**a**) Typical topology of a IEEE-33bus RDN [45], (**b**) Typical topology of a IEEE-69-bus RDN [45].

Table 1. LCPLI for IEEE-33-BUS RDN.

Bus	Initial Loading (MW)	Loading Capacity to Power Loss Index (LCPLI)
2	0.1	9.81
3	0.09	3.76
4	0.12	2.36
5	0.06	1.67
6	0.06	1.04
7	0.2	0.95
8	0.2	0.55
9	0.06	0.45
10	0.06	0.37
11	0.045	0.36
12	0.06	0.34
13	0.06	0.28
14	0.12	0.26
15	0.06	0.25
16	0.06	0.23
17	0.06	0.20
18	0.09	0.19
19	0.09	9.55
20	0.09	7.38
21	0.09	6.97
22	0.09	6.38
23	0.09	3.60
24	0.42	3.37
25	0.42	3.19
26	0.06	1.01
27	0.06	1.01
28	0.06	0.97
29	0.12	0.95
30	0.2	0.94
31	0.15	0.91
32	0.21	0.91
33	0.06	0.91

Accommodation Profile of PEVs at Different SoC and Battery Capacity

The PEV is a stochastic load and needs special attention. The energy consumption of PEVs highly depends on the current SoC and battery capacity. Therefore, the presented study develops the accommodation profile of PEVs based on four battery capacities and seven SoC obtained [29,46]. The results indicate that 1297 units of PEVs can safely be accommodated (without violating constraints presented in Equations (11) to (14) when the battery capacity is highest (75 kWh) and SoC is 10% (least for assumed cases). However, with the decrease in battery capacity for the same SoC (10%), 3810 units of PEVs can safely be accommodated on the best bus location (bus-2).

Similarly, when the SoC and battery capacity are increased to maximum (70% for assumed cases), bus-2 can accommodate 10,334 PEVs. Similarly, the accommodation increases to 31,988 units for the same SoC when the battery capacity is lowest (24.2 kWh) among the assumed cases. The analysis indicates that the PEVs can be accommodated in the range of 1297 units to 31,988 units depending on battery capacity and SoC. The accommodation of PEVs enhances with the increase in SoC and decline in battery capacity since lower energy is required to charge the battery of PEVs. Similarly, the accommodation of PEVs decreases with the decrease in SoC and increase in battery capacity since a higher amount of energy is required to charge the battery. The accommodation profile of PEVs at a different SoC and battery capacities is depicted in Figure 7.

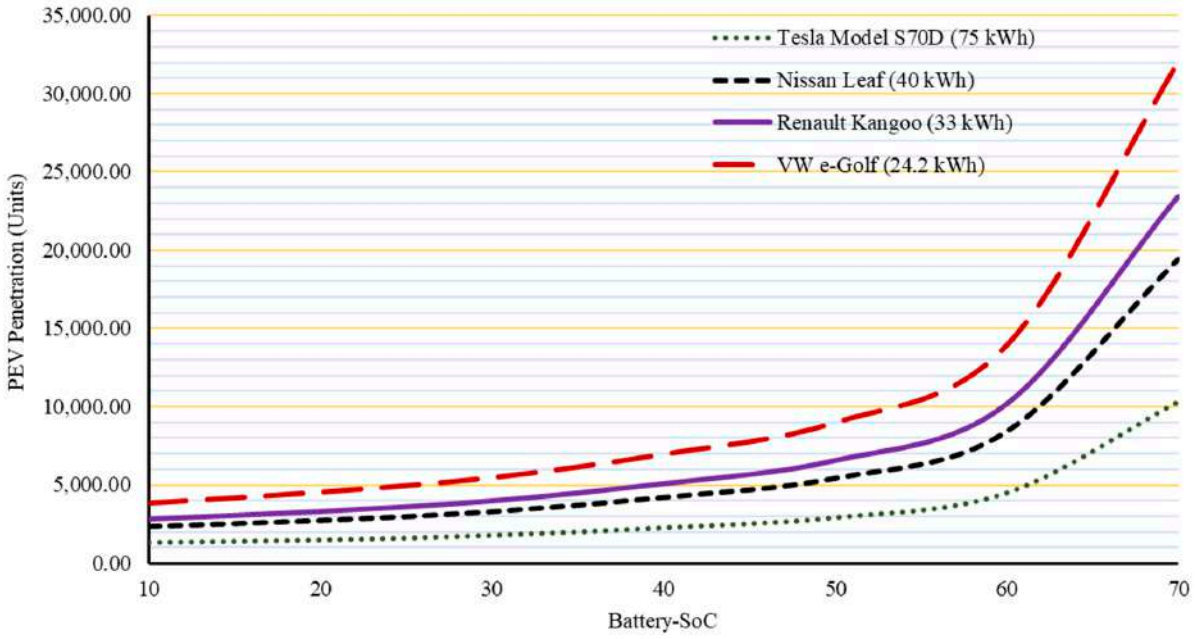

Figure 7. Penetration profile of PEVs.

3.2. Distributed Generation Allocation with Maximum PEV Load on Best Bus Location

After the PEVs are allocated on the best bus location, the DGs are properly allocated. In the PEV integrated network, the optimal size and location of DG units play a vital role to minimize active power losses in RDNs. The power losses depend on DG size and location and are considered decision variables [47,48]. To reduce power losses, the sizes and positions of the DG units are optimized using AOA, SSA, PSO, and hybrid SSAPSO and AOASSA. The standard AOA results in the least power losses among the standard algorithms compared with SSA and PSO.

Among the hybrid algorithms, SSAPSO and AOASSA result in the same power losses with the allocation of one DG unit. The AOA results highlight a DG of 2425 kW at bus number 26, SSA highlights a DG of 2528.3 kW at bus number 26, and PSO results highlight a DG of 2551.2 kW at bus-26, all of which produce minimum active power losses. Among the hybrid algorithms, SSAPSO and AOASSA results highlight that a DG of 2682.5 kW at bus-6 produces minimum power losses in the PEV integrated network.

The optimal allocation of two DG units indicates that the AOA results in fewer power losses than the standard SSA and PSO. The AOA suggests that an optimal size of 906.6 kW at bus-14 and 1113.2 kW at bus-30 results in minimum power losses. Alternatively, SSA and PSO results highlight that a DG number 1 of 697.6 kW and 1006.6 kW installed at bus locations 14 and 11 and a DG number 2 of 1115.6 kW and 1113.2 kW installed at bus number 30 and 31 produce minimum power losses. The hybrid SSAPSO and AOASSA indicate that the power losses are minimal when DGs of 1190.1 kW at bus-30 and 867.03 kW at bus-13 are installed.

Similarly, when three DG units are allocated, the standard AOA results in minimum power losses compared with the standard SSA and PSO. The analysis indicates that the highest power loss reduction (of 65.36%) is produced using the hybrid AOASSA with the allocation of three DG units. The performance of the hybrid AOASSA is the same compared with SSAPSO with allocating one or two DG units. However, the performance of the hybrid AOASSA is significantly higher compared with contending algorithms when three DG units are allocated. The power losses and associated DG sizes and locations obtained with different numbers of DG units allocated using various algorithms are presented in Table 2.

Table 2. Performance of proposed AOASSA.

Number of DG Units Allocated	Optimization Technique	DG Size, kW (@Bus Location)	Power Loss (kW)	PLR (%)
Without DG allocation (integration of maximum PEV load)	-	-	224.43	
1 DG unit allocation	AOA	2425(26)	118.05	47.40
	SSA	2528.3(26)	119.5	46.75
	PSO	2551.2(26)	120.7	46.21
	SSAPSO	2682.5(6)	117.13	47.81
	AOASSA	2682.5(6)	117.13	47.81
2 DG unit allocation	AOA	906.6(14), 1113.2(30)	95.31	57.53
	SSA	697.6(14), 1115.6(30)	96.54	56.98
	PSO	1006.6(11), 1113.2(31)	96.82	56.86
	SSAPSO	1190.1(30), 867.03(13)	94.69	57.80
	AOASSA	1190.1(30), 867.03(13)	94.69	57.80
3 DG unit allocation	AOA	723.54(14), 1228.2(30), 996.59(24)	78.73	64.92
	SSA	800(13), 980(24), 900(30)	79.67	64.50
	PSO	810(13), 1300(30), 810(24)	80.47	64.14
	SSAPSO	840.82(13), 1067(24), 1091.5(30)	77.94	65.27
	AOASSA	1184.6(24), 1077.2(30), 812.97(13)	77.74	65.36

3.3. Statistical Characteristics of Proposed AOASSA Algorithm

The metaheuristic algorithms are stochastic, and the output of algorithms change after each run. The reliability or robustness of an algorithm is checked with the statistical characteristics (which usually include mean, the best value, standard deviation, and variance) after multiple runs. The proposed AOASSA and other contending algorithms run 30 times to check the superiority of the algorithms. The proposed AOASSA and contending algorithms run 30 times to allocate DG units and minimize power losses in PEV integrated networks. The analysis indicates that the standard AOA results in minimum power losses, mean value, standard deviations, and variance among the standard algorithms. However, the power loss values, mean values, standard deviations, and variance are still higher than hybrid combinations. Among the hybrid combinations, the hybrid AOASSA results in least power loss value, mean value, standard deviation, and variance (after 30 individual runs). The results and statistical analysis after 30 individual runs for the proposed AOASSA and other contending algorithms in PEV integrated networks are presented in Table 3.

Table 3. Statistical superiority of proposed AOASSA.

Number of DG Units Allocated	Technique	Mean Power Loss (kW) $\overline{x}$	Standard Deviation σ	Variance σ^2
1 DG unit allocation	AOA	124.71	4.31	18.55
	SSA	126.01	5.18	26.85
	PSO	127.42	5.30	28.08
	SSAPSO	119.90	1.63	2.66
	AOASSA	117.97	0.78	0.61
2 DG unit allocation	AOA	100.41	4.39	19.29
	SSA	101.24	5.25	27.59
	PSO	102.76	5.44	29.58

Table 3. *Cont.*

Number of DG Units Allocated	Technique	Mean Power Loss (kW) $\bar{x}$	Standard Deviation σ	Variance σ^2
2 DG unit allocation	SSAPSO	96.59	2.39	5.69
	AOASSA	95.31	1.14	1.30
3 DG unit allocation	AOA	83.58	4.42	19.51
	SSA	86.54	5.35	28.64
	PSO	87.74	6.04	36.43
	SSAPSO	81.07	2.45	6.00
	AOASSA	78.50	1.53	2.35

3.4. Convergence Characteristics of Proposed AOASSA Algorithm

The convergence behavior of an algorithm describes how it conducts its search during the optimization process. The algorithms begin by selecting an appropriate area to search within, with a large moment of particles (exploration phase), and then proceed with a lower moment in that search area (exploitation phase). Furthermore, the algorithms either suffer from exploration or exploitation capabilities. In the proposed study, the SSA works well in the exploration phase but lacks in the exploitation phase. The AOA works well in the exploitation phase but suffers from exploration capabilities. The results indicate that the AOA converged at 118.05 kW (47.40%), the SSA converged at 119.5 kW (46.75%), and the PSO converged at 120.7 kW (46.21%), with an optimal allocation of one DG unit after 200 iterations. Among the hybrid combinations, the SSAPSO and AOASSA are strong enough to search optimal size and locations of DG units. The results show that both the SSAPSO and AOASSA algorithms found the same value of minimum power loss in the network integrated with PEVs. Specifically, the two algorithms both reached a power loss of 117.13 kW with the optimal placement of a single DG unit. The performance of the proposed AOASSA algorithm is compared with other competing algorithms in terms of their convergence characteristics, with the results presented in Figure 8 when only one DG unit is used.

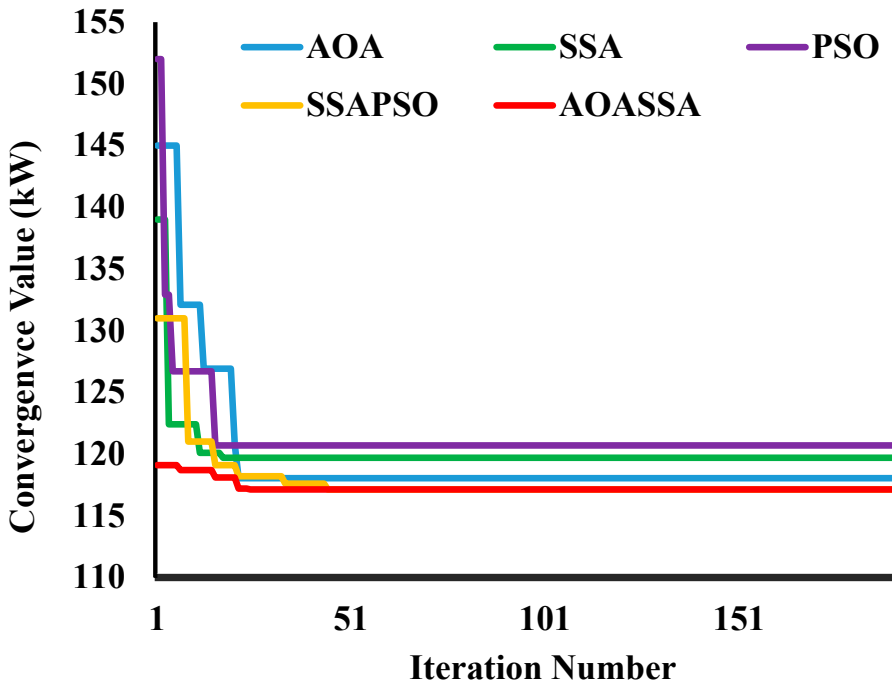

Figure 8. Convergence characteristics with one DG unit allocation.

The power loss results are also evaluated using the optimal placement of two DG units. The results indicate that the AOA significantly reduces power losses compared with contending standard algorithms. The proposed AOA converged to a power loss value of 95.31 kW (PLR of 57.53%), the SSA converged at 96.54 kW (56.98%), and the PSO converged at 96.82 kW (56.86%). In comparison with the SSA and PSO, the outcomes shows that the AOA produces the highest power loss reduction. However, compared with hybrid combinations, the standard AOA still results in higher power losses. The hybrid SSAPSO and AOASSA converged to a 94.69 kW power loss value (PLR of 57.80%), which is significantly lower than the standard AOA, SSA, and PSO. The study suggests that the AOASSA and SSAPSO algorithms have similar results in terms of power loss reduction when two DG units are allocated optimally. The convergence of the two algorithms with the optimal allocation of two DG units is shown in Figure 9.

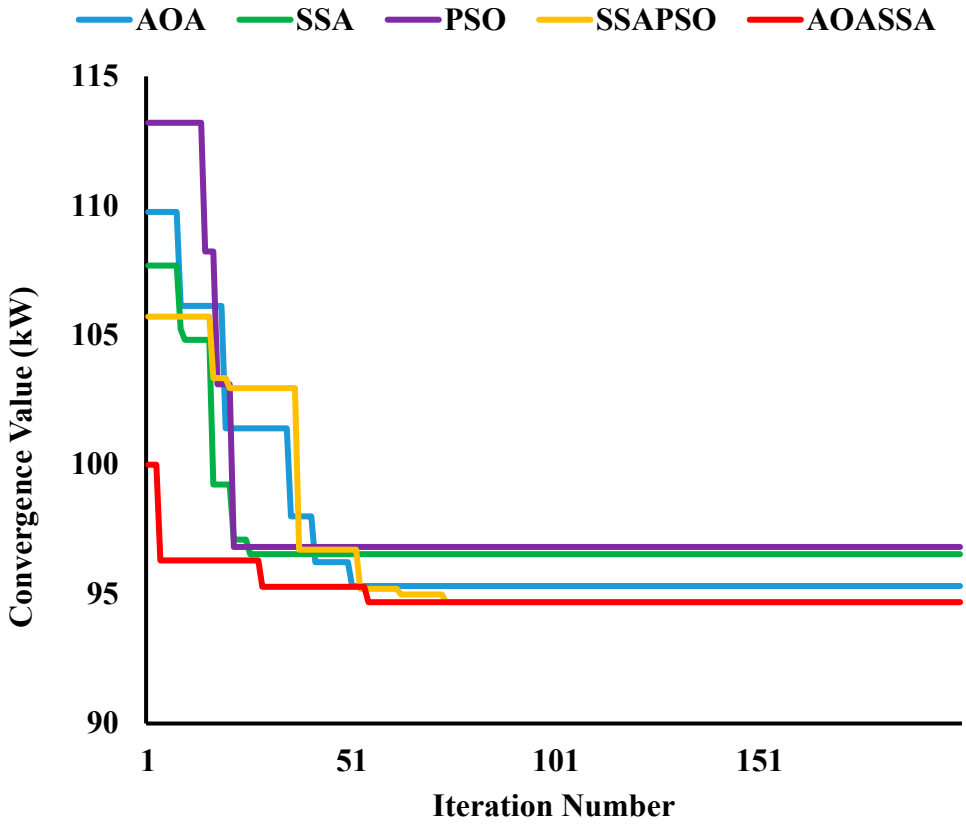

Figure 9. Convergence characteristics with two DG unit allocation.

Similarly, three DG units are allocated, and the convergence characteristics are analyzed during the search process. The analysis indicates that the performance of the standard AOA is superior compared with the standard SSA and PSO. The results demonstrate that the AOA converged to a PLR of 64.92%, the SSA converged to a PLR of 64.50%, and the PSO converged to PLR of 64.14%. Amid the standard algorithms, the highest PLR is produced by using a standard AOA. However, unlike the convergence characteristics of one and two DG allocation, the hybrid AOASSA performs better than the SSAPSO. The hybrid SSAPSO produces a PLR of 65.27% while the hybrid AOASSA produces a power loss of 65.36%. The performance of the proposed AOASSA is significantly higher than other contending algorithms. The convergence characteristics of the proposed AOASSA and other contending algorithms in PEV integrated networks is presented in Figure 10.

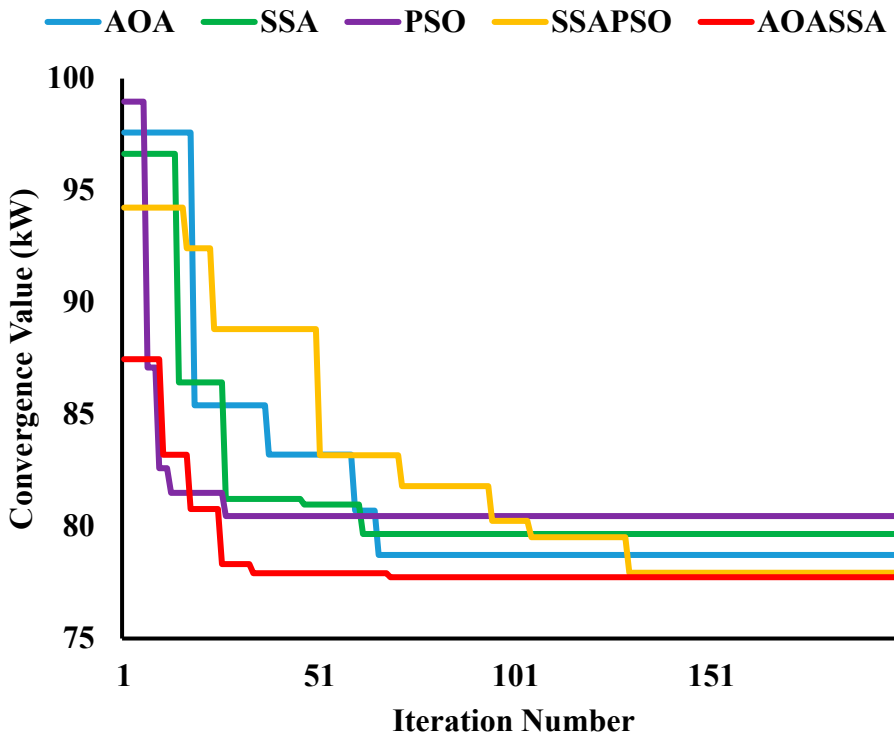

Figure 10. Convergence characteristics with three DG unit allocation.

3.5. PEV Charge and Discharge Ratio Optimization for Power Loss Reduction

PEVs operate in two modes of operation (i.e., charging and discharging). In the charging mode of PEVs (G2V), the PEVs consume energy from the grid, while in the discharging mode (V2G), the PEVs supply energy to the grid. The proposed study develops a methodology to optimize the charge and discharge ratios of PEVs that results in minimum power losses. The charging and discharging of PEVs place a net load on the system. The net load is the difference between the charging load of PEVs, the conventional, and the supply from PEV (vehicle to grid—V2G). In other words, the net load is controlled by utility operators to minimize the power losses in RDNs. Therefore, it is not necessary that 100% discharging of PEVs results in minimum power loss, since the distribution networks are nonlinear. The proposed study develops a mechanism to optimize the charge and discharge ratios of PEVs, even if the DG sizes and locations are fixed.

3.5.1. Charge and Discharge Ratio Optimization with One DG Unit Allocation

Initially, the power losses are minimized with charge and discharge ratios of PEVs in the presence of the maximum load of PEVs on best bus location and optimal allocation of one DG unit. The PEV load of 2.2 MW is placed on bus-2 (since 2.2 MW is the maximum load of PEVs and bus-2 is selected since bus-2 results in the highest LCPLI). The DG unit of 2682.5 kW is placed on bus-6 (the optimum allocation of one DG unit). The maximum loading of PEVs is divided into ten segments (as described in Section 2) and ten cases are generated based on the charging and discharging of PEVs. The power losses are calculated using load flow analysis in different charging and discharging scenarios. Initially, when 10% PEVs are discharged and 90% PEVs are charged, the power losses are reduced from 224.43 kW to 115.48 kW (48.54% reduction). The power losses vary between 115.48 kW and 110.22 kW (50.88% reduction) based on the charging and discharging ratios of PEVs. The minimum power losses are achieved when 20% PEVs are charged and 80% PEVs are discharged. The net load on the best bus location (i.e., bus-2) produces the least power losses of 110.22 kW in the presence of one DG unit allocation. The power losses for various charge and discharge ratio profiles are depicted in Figure 11.

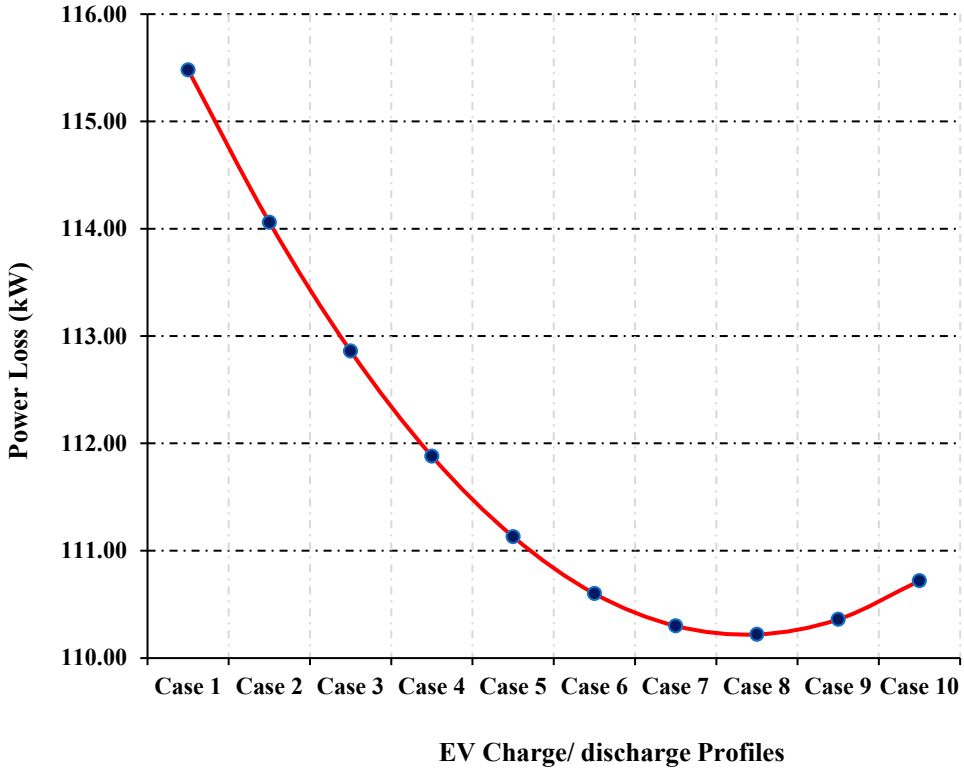

Figure 11. Charge and discharge ratios of PEVs against power loss in presence of 1 DG unit.

The charge and discharge ratios are imperative to optimize since this allows local distribution companies to minimize power losses even in the presence of fixed PEV and DG allocation. The charging/discharging of PEVs and the nature of the distribution network are nonlinear. Therefore, the optimal operation point is crucial for a distribution system operator. In the presence of one DG unit (optimal size and location), the optimal charge and discharge ratios are 20% and 80%, respectively, since power losses increase as the charging and discharging ratios changes.

Furthermore, the power losses change exponentially with the change in charging and discharging of PEVs. The reason is that the PEVs batteries are exponential and hence the battery characteristics are observed.

3.5.2. Charge and Discharge Ratio Optimization with Two DG Unit Allocation

Similar to one DG unit allocation, the power losses vary with the change in charge and discharge ratios of PEVs and the number of DG units allocated. The power losses against the charge and discharge ratios of PEVs in the presence of two DG units (optimal allocation) is depicted in Figure 12. The charge and discharge ratios are again segmented into ten equal divisions in the presence of two optimal sizes and locations of DGs. The allocated sizes and locations of DGs are assumed for the AOASSA only since it results in minimum power losses. The DG size 1 of 1190.1 kW and DG size 2 of 867.03 kW are located.

On the best bus location, the charge and discharge ratios are changed to obtain minimum power losses. The power losses vary from 92.75 kW (58.76%) to 85.29 kW (62%) with the variation in charge and discharge ratios of PEVs. The minimum power losses are achieved with 90% discharging of PEVs and 10% charging of PEVs. The optimal charge and discharge ratios change with the number of DG units allocated since the power injection changes from the best bus location (bus-2).

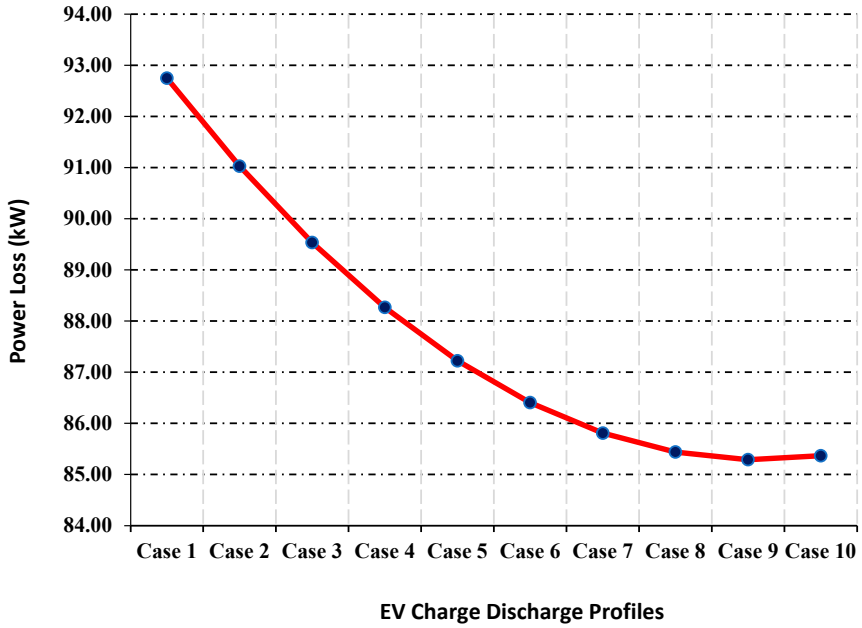

Figure 12. Charge and discharge ratios of PEVs against power loss in presence of 2 DG units.

3.5.3. Charge and Discharge Ratio Optimization with Three DG Unit Allocation

The optimal charge and discharge ratios vary with the number of DG units allocated. The PEV load is segmented into ten parts and the power losses are observed at different charge and discharge ratios of PEVs. The power losses vary between 76.34 kW and 72.59 kW. The least power losses are achieved when 70% PEVs are discharged and 30% PEVs are charged in the presence of three DG units allocated. The power losses at different charge and discharge ratios in the presence of three DG units are depicted in Figure 13.

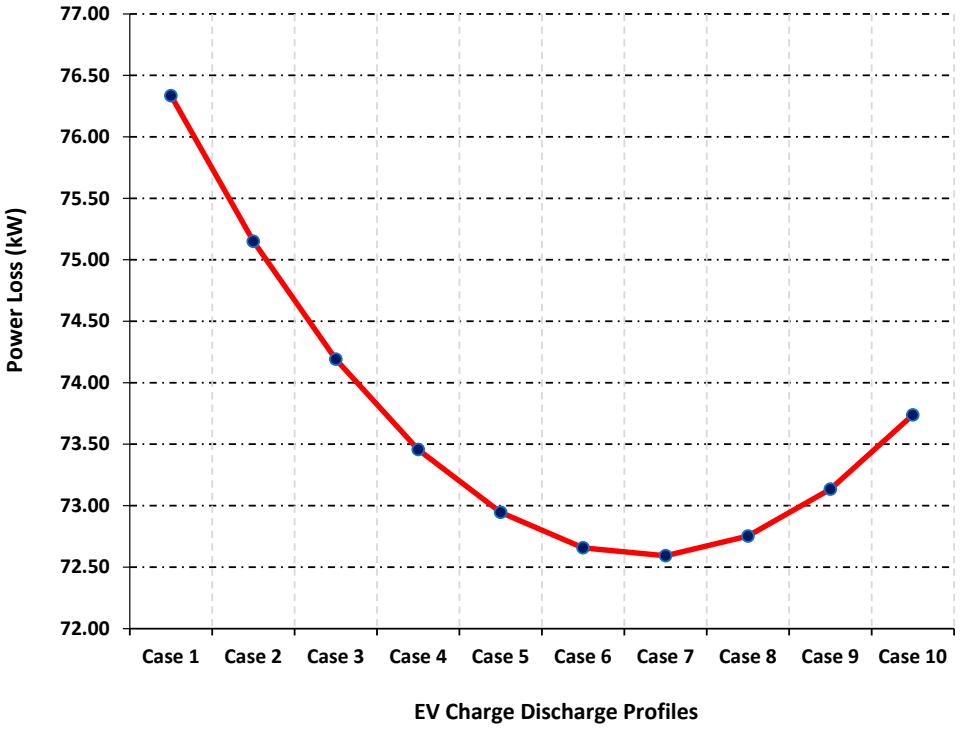

Figure 13. Charge and discharge ratios of PEVs against power loss in presence of 3 DG units.

3.6. Selection of Best Bus for Accommodating PEVs Based on LCPLI in IEEE69-Bus RDN

The proposed study accommodates the PEVs lumped into a single bus. The selection of the best bus is based on the LCPLI. The bus with maximum loading capacity (referring to the violation of constraints) and minimum power losses at maximum loading is the best bus to accommodate the PEVs. The maximum loading on the individual bus is checked with the variation in loading capacity and the corresponding power losses are noted. Each bus is varied with a step size of 0.1 MW and the distribution network constraints are checked with the corresponding increase in loading. The ratio of maximum loading capacity to the corresponding power losses (LCPLI) for the 69-bus network (bus-1 is not considered since bus-1 is a slack bus) is presented in Table 4.

Table 4. LCPLI for 69-bus network.

Bus	Initial Loading (MW)	Loading Capacity to Power Loss Index (LCPLI)
2	0	28.24
3	0	28.20
4	0	28.06
5	0	26.40
6	0.0026	10.79
7	0.0404	5.69
8	0.075	5.08
9	0.03	4.84
10	0.028	4.40
11	0.145	4.31
12	0.145	4.03
13	0.008	3.74
14	0.008	3.48
15	0	3.25
16	0.0455	3.21
17	0.06	3.12
18	0.06	3.12
19	0	3.02
20	0.001	2.96
21	0.114	2.87
22	0.0053	2.87
23	0	2.83
24	0.028	2.75
25	0	2.60
26	0.014	2.54
27	0.014	2.51
28	0.026	28.02
29	0.026	25.73
30	0	17.94
31	0	17.03
32	0	13.56
33	0.014	9.07
34	0.0195	6.04
35	0.006	5.29
36	0.026	28.02
37	0.026	25.68
38	0	22.84
39	0.024	22.14
40	0.024	22.10
41	0.0012	13.05
42	0	11.18
43	0.006	10.97
44	0	10.93
45	0.0392	10.42

Table 4. *Cont.*

Bus	Initial Loading (MW)	Loading Capacity to Power Loss Index (LCPLI)
46	0.0392	10.42
47	0	27.90
48	0.079	24.34
49	0.3847	17.32
50	0.3847	16.18
51	0.0405	5.07
52	0.0036	4.95
53	0.0044	4.13
54	0.0264	3.52
55	0.024	2.89
56	0.024	2.90
57	0	2.48
58	0	1.34
59	0	1.09
60	0.1	1.02
61	0	0.93
62	1.244	0.84
63	0.032	0.83
64	0	0.81
65	0.227	0.73
66	0.059	0.65
67	0.018	4.26
68	0.018	4.26
69	0.028	3.88

The LCPLI for the 69-bus network is determined using an analytical method. The LCPLI is found to be highest for bus-2, -3 and -4. Among the top three buses, the bus with the highest LCPLI is bus-2. The second number bus achieves a highest LCPLI of 28.24 units, while bus-3 achieves a slightly reduced LCPLI of 28.19 units. Therefore, the best bus to accommodate PEVs is bus-2.

Accommodation Profile of PEVs at Different SoC and Battery Capacity in 69-Bus

The PEV load is stochastic in nature and the accommodation profile of PEVs depends upon the battery capacity and state of charge. In order to deal with the stochasticity of the PEVs, the proposed study considers four battery capacities and seven states of charge. The accommodation profile of PEVs is developed considering various SoC and BCs. Initially, when the SoC is least (10%) and the battery capacity is highest (75 kWh), the best bus can accommodate 3752 units of PEVs. Considering the same SoC and a decrease in battery capacity to 24.2 kWh, the accommodation of PEVs increases to 11,019 units. Alternatively, the current SoC significantly impacts the accommodation profile of PEVs. When the SoC increases to 70% (highest among the assumed cases), the best bus can accommodate 29,890 units of PEVs for the 75 kWh battery pack. The best bus can accommodate a highest of 92,519 units of PEVs when the SoC is highest (70%) and the battery pack is lowest (24.2 kWh) among the assumed stochastic battery capacities and SoC. Therefore, the analysis reveals that the best bus accommodates 3752 to 92,519 units of PEVs on the best bus location. The accommodation of PEVs is found to be dependent on the SoC and BC. The stochastic analysis of PEVs indicates that the battery capacity and SoC significantly impact the accommodation of PEVs. The analysis of PEV accommodation indicates that the accommodation of PEVs increases with the increase in the current SoC. Alternatively, the accommodation of PEVs decreases with the increase in battery capacity. The accommodation profile of PEVs at different SoC and battery capacities is presented in Figure 14.

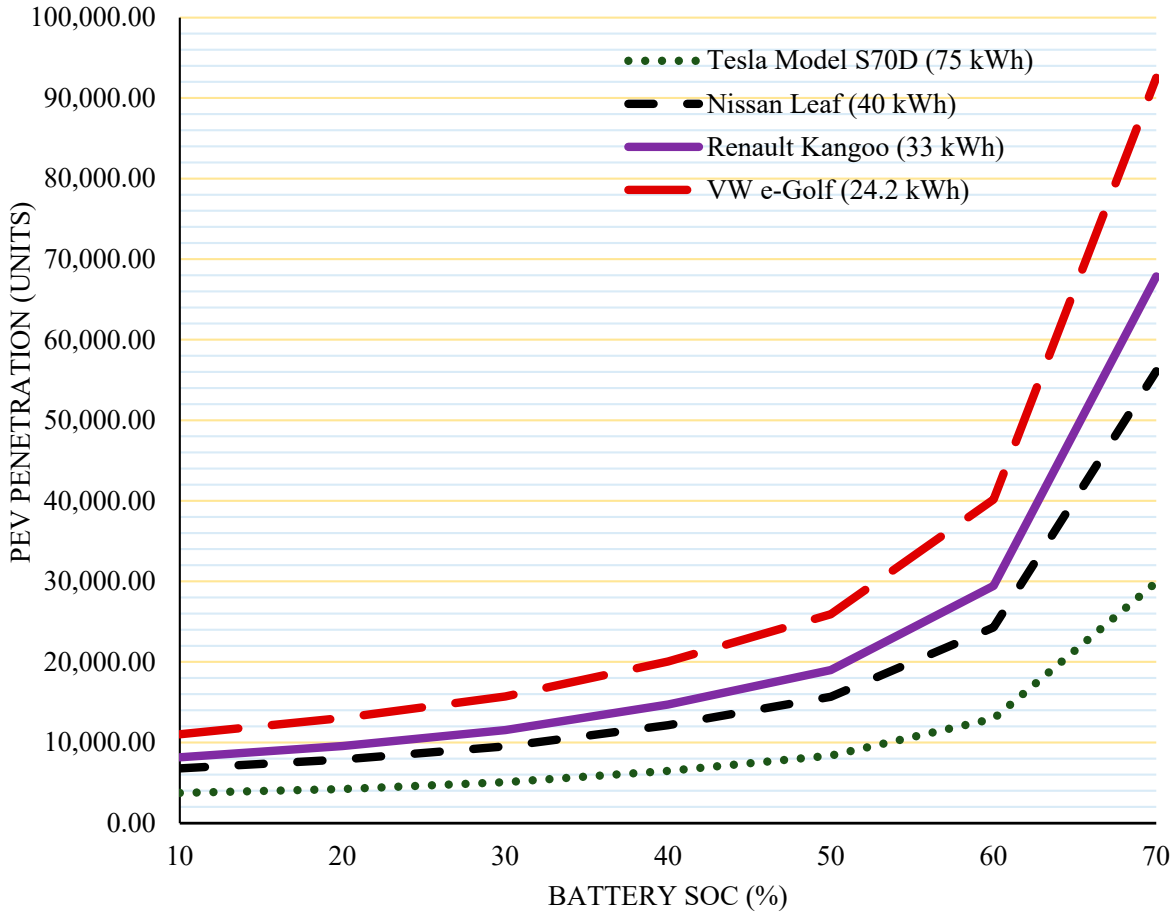

Figure 14. Accommodation profile of PEVs in IEEE-69-bus RDN.

3.7. Distributed Generation Allocation with Maximum PEV Load on Best Bus Location in IEEE-69-Bus RDN

After the optimal allocation of PEV units, the DG size and location are optimized to minimize the power losses in radial distribution networks. The optimal allocation of DG units is a combinatorial problem involving discrete and variables. Therefore, DG allocation is a complex combinatorial and nonlinear optimization problem. The complex DG allocation optimization problem requires advanced optimization techniques to minimize the power losses in the distribution network integrated with the maximum PEV load on the best bus location. Initially, the standard AOA, SSA, PSO, SSAPSO, and AOASSA are applied to determine optimal size and location of one DG unit that results in minimum power losses. The results reveal that the optimal allocation of one DG unit produces power loss reductions of 62.93%, 62.54%, and 61.96% when the standard AOA, SSA, and PSO are applied, respectively. However, the standard AOA, SSA, and PSO suffer from inherent deficiencies and produce higher power losses in comparison with the hybrid SSAPSO and AOASSA. The hybrid SSPASO and AOASSA produce a higher power loss reduction of 62.96% with the optimal allocation of one DG unit.

Then, the optimal sizing and locations of two DG units are determined with the integration of the maximum PEV load on the best bus location. The standard AOA, SSA, PSO, and hybrid combinations of SSAPSO and AOASSA are implemented to determine optimal size and location to achieve minimum power losses. The results reveal that the power loss reduction produced by the standard AOA, SSA, and PSO are 68.02%, 67.47%, and 66.92%, respectively. However, the hybrid SSAPSOA and AOASSA are capable of producing a higher power loss reduction. The hybrid SSAPSO and AOASSA produce the highest power loss reduction of 68.10% with the optimal sizes and locations of two DG units.

Finally, the optimal allocation of three DG units is considered for power loss minimization in IEEE-69-bus radial distribution networks. The optimal allocation of three DG units is a complex problem in comparison with the optimal allocation of two DG units. The optimal allocation of three DG units involves three DG sizes and three DG locations (six decision variables) to minimize power loss reduction. The standard AOA, SSA, PSO, SSAPSO, and AOASSA are implemented to obtain optimal sizes and locations of three DG units for minimization of power losses. The results reveal that the standard AOA produces a power loss reduction of 68.53%, the SSA produces a power loss reduction of 67.96%, and the PSO produces a power loss reduction of 67.30% with optimal allocation of three DG units. However, the hybrid SSAPSO produces a power loss reduction of 68.85% and the hybrid AOASSA produce the highest power loss reduction of 69.10% with the optimal allocation of three DG units.

The results conclude that the power losses reduce with the increase in number of DG units allocated. Furthermore, the standard AOA produces the highest power loss reduction in comparison with the standard SSA and standard PSO. However, the power loss reduction produced by the hybrid SSAPSO and AOASSA is the same with the optimal allocation of one and two DG units. The power loss reduction produced by the hybrid AOASSA is slightly higher than the SSAPSO when 3 DG units are allocated. The performance superiority of the proposed AOASSA is evident when the number of decision variables (sizes and locations of DG units in DG allocation problem) increases. The optimal size/sizes and location/locations of one, two, and three DG units and the corresponding power losses are presented in Table 5.

Table 5. Performance of proposed AOASSA on 69-bus RDN with multiple DGs.

Number of DG Units Allocated	Optimization Technique	DG Size, kW (@Bus Location)	Power Loss (kW)	PLR (%)
Without DG allocation (integration of maximum PEV load)	-		225.3	
1 DG unit allocation	AOA	1829.10@61	83.50	62.93
	SSA	2039.70@61	84.39	62.54
	PSO	2130.0@61	85.69	61.96
	SSAPSO	1873.20@61	83.43	62.96
	AOASSA	1873.20@61	83.43	62.96
2 DG unit allocation	AOA	1778.2@61, 554.91 @15	72.03	68.02
	SSA	1589@61, 576 @15	73.27	67.47
	PSO	1922.20@61, 755.50 @15	74.52	66.92
	SSAPSO	1781.90@61, 531.90 @17	71.87	68.10
	AOASSA	1781.90@61, 531.90 @17	71.87	68.10
3 DG unit allocation	AOA	1702.6@61, 524.63@67, 229.03@18	70.91	68.53
	SSA	393.1@67, 629@18, 1577.8@61	72.17	67.96
	PSO	401@67, 726.19@18, 1640@61	73.67	67.30
	SSAPSO	452.77@17, 1689@61, 678.06@18	70.17	68.85
	AOASSA	528.32@11, 380.35@18, 1719.2@61	69.60	69.10

3.8. Statistical Characteristics of Proposed AOASSA Algorithm

The optimal allocation of DG units is a combinatorial optimization problem involving discrete and continuous variables. The optimal allocation of DG units requires advance algorithms to minimize power losses in radial distribution networks. The metaheuristic and hybrid metaheuristic algorithms are stochastic in nature, and the power losses produced

in an individual run are not same. The algorithms start with the random generation of size/sizes and location/locations and update the solution with the inherent mechanism. The robustness of an algorithm is checked with the statistical characteristics obtained after multiple runs. The statistical characteristics involve mean value, standard deviations, and variance of power losses. The standard AOA, SSA, PSO, and hybrid SSAPSO and AOASSA run 30 times individually to check the robustness of the algorithms. The results reveal that the standard AOA produces the least mean power losses, standard deviation, and variance at the end of 30 individual runs. However, among the hybrid combinations, the AOASSA produces the least mean value of power losses, standard deviations, and variance at the end of 30 individual runs. The results of mean power loss value, standard deviations, and variance with multiple DG unit allocations are presented in Table 6.

Table 6. Statistical superiority of proposed AOASSA in 69-bus RDN.

Number of DG Units Allocated	Technique	Mean Power Loss (kW) $\bar{x}$	Standard Deviation σ	Variance σ^2
1 DG unit allocation	AOA	87.94	4.44	19.79
	SSA	90.54	5.65	32.01
	PSO	91.95	5.81	33.81
	SSAPSO	85.45	2.49	6.24
	AOASSA	84.27	0.98	0.96
2 DG unit allocation	AOA	76.59	4.59	21.07
	SSA	79.69	5.79	33.61
	PSO	80.39	5.98	35.80
	SSAPSO	74.91	2.70	7.33
	AOASSA	74.08	1.36	1.85
3 DG unit allocation	AOA	75.94	4.61	21.27
	SSA	78.34	5.97	35.74
	PSO	80.20	7.49	56.25
	SSAPSO	74.39	3.00	9.05
	AOASSA	71.65	2.13	4.57

3.9. Convergence Characteristics of Proposed AOASSA Algorithm in IEEE-69 -Bus RDN

The convergence characteristics of an algorithm describe the searching pattern of an individual algorithm in a search space. A good optimization algorithm generates more diverse particles during the exploration phase of the search process and relatively less diverse particles during the search process's later stages (exploitation). The standard AOA, SSA, PSO, and hybrid SSAPSO and AOASSA run 200 iterations in a single run and update the power losses. Initially, the AOA, SSA, PSO, SSAPSO, and AOASSA run 200 iterations to allocate one DG unit optimally for power loss minimization. The results reveal that the standard AOA produces power loss reduction of 57.83%, the standard SSA produces a power loss reduction of 58.63, and the PSO produces a power loss reduction of 57.16% in the first iteration. The standard AOA, SSA, and PSO produce a power loss reduction of 62.93%, 62.54%, and 61.96%, respectively. A power loss decrease of 62.96% is achieved using the combination SSAPSO and AOASSA. The convergence characteristics of one DG unit allocation achieved using AOA, SSA, PSO, SSAPSO, and AOASSA in the IEEE-69 bus RDN are shown in Figure 15.

Similar to the allocation of one DG unit, the algorithms are implemented for the allocation of two DG units and the convergence characteristics of the best run are presented. The results reveal that the standard SSA has good exploration capabilities and the AOA has good exploitation capabilities. The standard AOA reduces the power loss to 61.60% in the first iteration, the standard SSA reduces the power loss to 62.98%, and the standard PSO reduces the power loss to 60.94% in the first iteration. However, the exploration capabilities of the hybrid SSAPSO and AOASSA are superior compared with the standard AOA. The hybrid SSAPSO and AOASSA reduce the power loss to 64.49% and 66.04%,

respectively, in the first iteration. The power loss value in the first iteration reflects the exploration capabilities of the algorithms. The algorithms retrieve values of power losses for 200 iterations. At the end of the search process, the standard AOA performs superior to the standard SSA and PSO. The AOA, SSA, and PSO converged to 68.02%, 67.47%, and 66.92% power loss reduction, respectively. However, the exploitation capabilities of the hybrid SSAPSO and AOASSA are superior compared with the standard AOA, SSA, and PSO. The SSAPSO and AOASSA converged to a 68.10% value of power loss with the allocation of two DG units at the end of 200 iterations. The convergence characteristics of two DG unit allocation in the PEV integrated 69-bus network is presented in Figure 16.

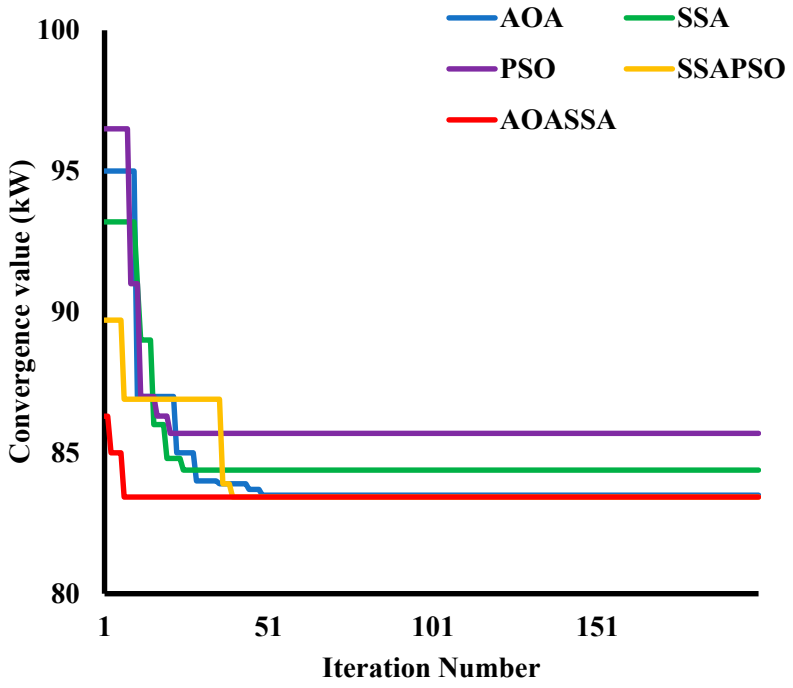

Figure 15. Convergence characteristics with one DG unit allocation.

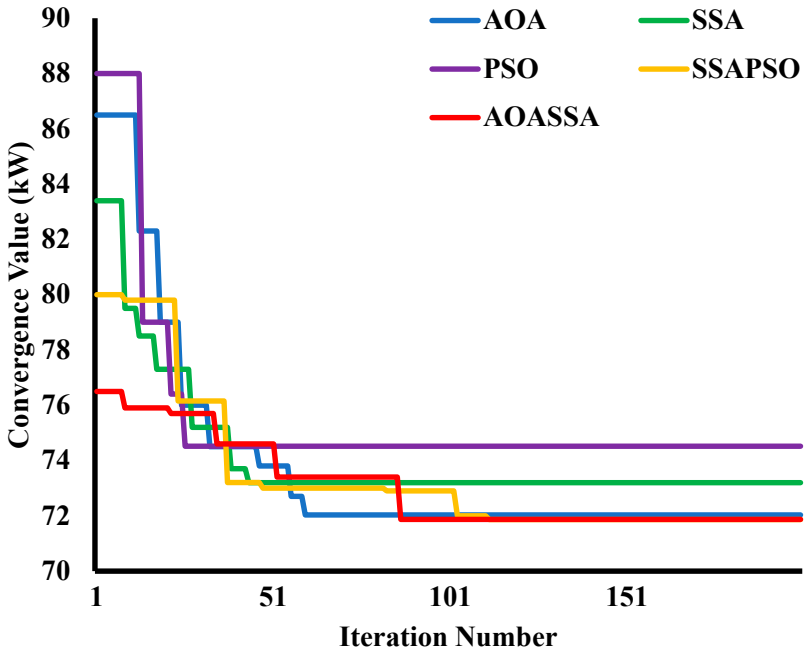

Figure 16. Convergence characteristics with two DG unit allocation.

Similar to one and two DG unit allocations, the convergence characteristics of three DG unit allocation is observed. The standard AOA, SSA, PSO, SSPAO, and AOASSA are applied for the allocation of three DG units, and the convergence characteristics of the best run are presented. The results reveal that the standard SSA exhibits superior exploration capabilities among the standard algorithms. The power loss obtained by AOA, SSA, and PSO in the first iteration are 63.73%, 64.40%, and 63.24%, respectively. However, the hybrid combination of SSAPSO and AOASSA are superior to the standard AOA, SSA, and PSO. The hybrid SSAPSO and AOASSA obtained a power loss of 65.69% and 66.75%, respectively, in the first iteration. The results also reveal that the standard AOA converged to a better power loss value than the standard SSA and PSO. The exploitation capabilities of the standard AOA are superior to the standard SSA and PSO. The standard AOA, SSA, and PSO converged to 68.53%, 67.96%, and 67.30% power loss values, respectively, at the end of 200 iterations. However, the hybrid combination of SSAPSO and AOASSA are superior to the standard AOA, SSA, and PSO algorithms. The hybrid SSAPSO converged to 68.85% power loss and the hybrid AOASSA converged to a 69.10% power loss value. The convergence characteristics of the hybrid AOASSA are superior to the contending algorithms. The convergence characteristics of three DG unit allocations in PEV integrated IEEE-69-bus networks are presented in Figure 17.

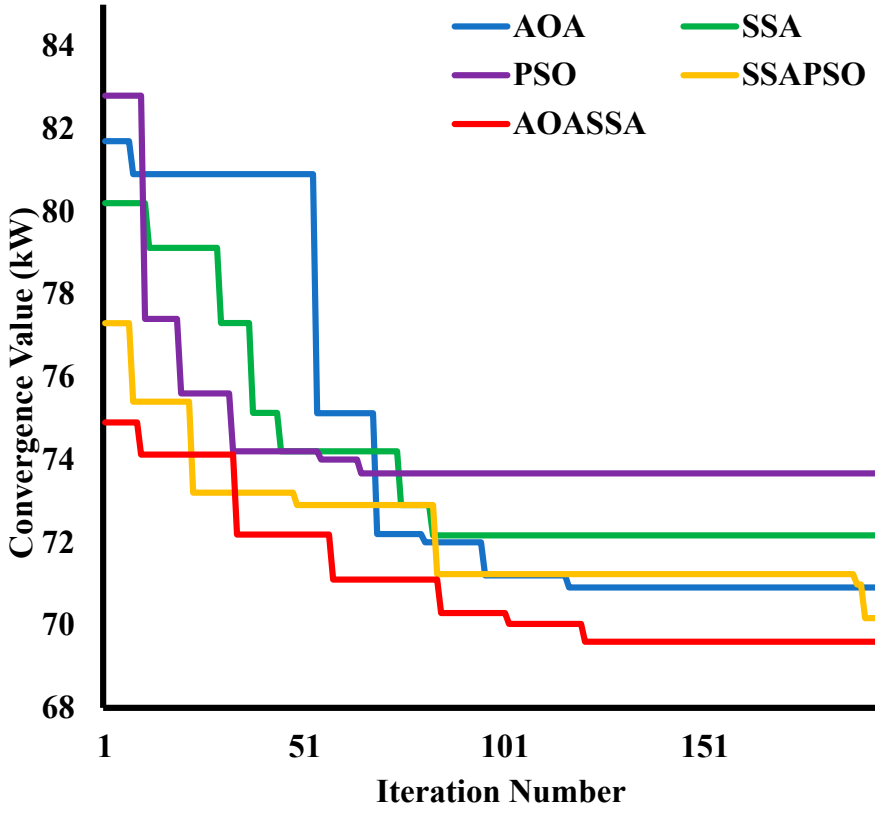

Figure 17. Convergence characteristics with three DG unit allocation.

3.10. PEV Charge and Discharge Ratio Optimization for Power Loss Reduction in IEEE69-Bus RDN

The PEVs act as a battery charging load or a battery discharging source. The PEVs consume energy from the grid when the PEVs act as a battery charging load. Alternatively, the PEVs supply energy when the PEVs act as a battery discharging source. The proposed study balances the charge and discharge ratios of PEVs, such that the net load on the system produce minimum power losses in a 69-bus RDN. The net load is the difference between the standard load of the bus, charging load of PEVs and the battery discharging power. The net load is controllable and the utility can allocate a net load that results in minimum power losses. The distribution network is nonlinear in nature and the charging and discharging of

PEVs have a significant impact on power losses of the network. Therefore, the power losses are highly dependent on the net load on the bus where the PEVs are allocated, and the net load is dependent on charging and discharging ratios of PEVs. The optimal charge and discharge ratios enable the utility operators to minimize the power losses when the sizes and locations of DG units are fixed. The optimal charge and discharge ratios are highly dependent on the number of DG units allocated. The optimal charge and discharge ratios change with the change in number of DG units allocated. The study develops the charging and discharging profiles of PEVs with one, two, and three DG units allocated at the optimal size and location.

3.10.1. Charge and Discharge Ratio Optimization with One DG Unit Allocation

The charge and discharge ratios of PEVs are optimized with the allocation of one DG unit and PEVs are placed at the optimal location. The best bus to accommodate PEVs is found to be bus-2, since bus-2 has the highest LCPLI of 28.24 units. The best bus has 6.36 MW of additional power to accommodate PEVs. The maximum loading is based on violation of RDN constraints. The DG unit of 1873.20 kW is also allocated at bus number 61. The proposed methodology divides the maximum loading into ten different cases, which are based on the charging and discharging of PEVs. The net load is placed on the best bus location, which is based on charging and discharging of PEVs and standard loading of the best bus location. The power losses are calculated using load flow analysis. Initially, 10% PEVs are discharged and 90% PEVs are charged. The power losses of the network are found to be 83.36 kW. The minimum power losses are not achieved when 100% PEVs are discharging. The minimum power losses of 83.20 kW are achieved when 70% PEVs are discharging and 30% PEVs are charging at the best bus location. The charging and discharging profile of PEVs against the IEEE-69-bus network power losses in the presence of one DG unit is depicted in Figure 18. The charging and discharging of PEVs enable the utility operators to minimize the power losses despite the DG unit being allocated at the optimal bus location. The optimal charge and discharge profile of PEVs is nonlinear in nature, since PEV load and RDN are also nonlinear in nature.

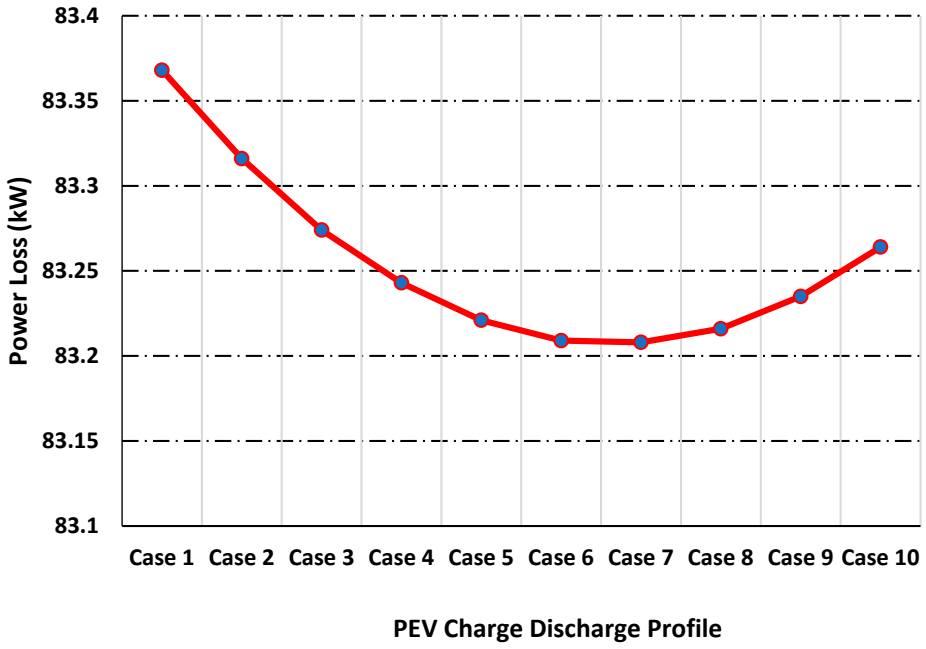

Figure 18. Charge and discharge ratios of PEVs against power loss in presence of 1 DG unit.

3.10.2. Charge Discharge Ratio Optimization with Two DG Unit Allocation

The optimal charge and discharge ratios vary with the variation in number of DG units allocated. The presence of two DG units at the optimal bus location change the net

loading of the network; therefore, the optimal charge and discharge ratios are also changed. The PEV loading is divided into ten different cases, which are based on charging and discharging of PEVs. The power losses of the IEEE-69 bus RDN vary between 71.67 kW and 71.86 kW, depending on the charging and discharging of PEVs. The minimum power loss of 71.67 kW is achieved when 60% PEVs are discharging and 40% PEVs are charging. The charging and discharging profile of PEVs against power losses of the 69-bus RDN in the presence of two DG units is depicted in Figure 19.

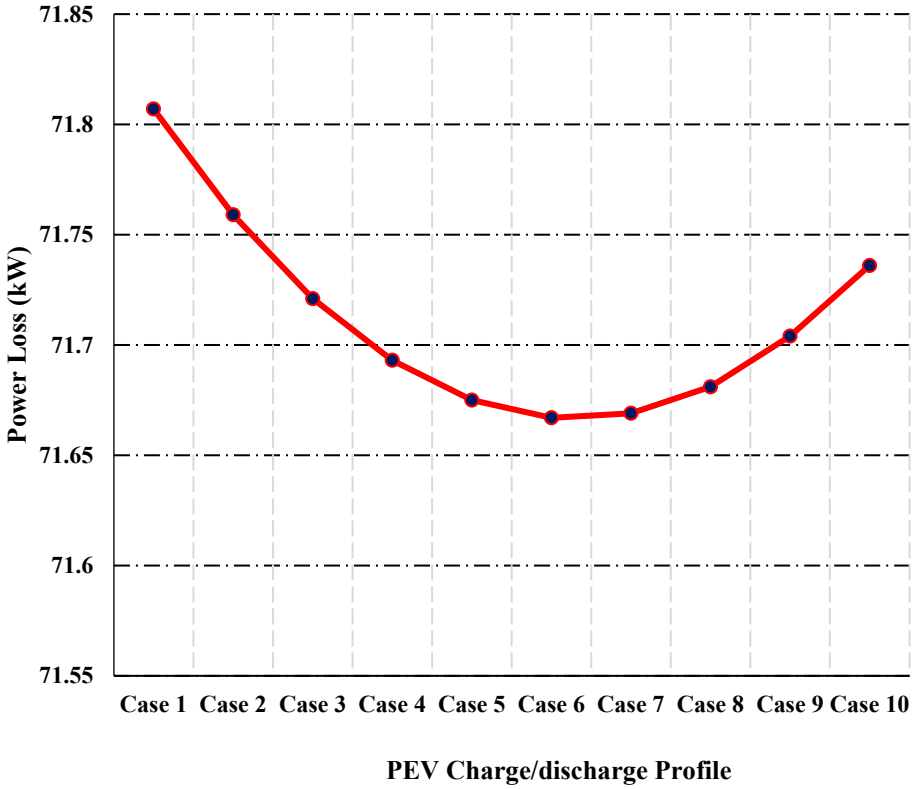

Figure 19. Charge and discharge ratios of PEVs against power loss in presence of 2 DG unit.

3.10.3. Charge and Discharge Ratio Optimization with Three DG Unit Allocation

The optimal charge and discharge ratios are highly dependent on the number of DG units allocated. The change in the number of DG units produces a corresponding change in the optimal charge and discharge ratios. The proposed methodology divides the PEV loading into ten cases, which are based on charging and discharging ratios of PEVs. The power losses of the 69-bus RDN vary between 69.42 kW and 69.60 kW depending on the charge and discharge ratios of PEVs. The optimal charge and discharge ratios of PEVs are 40% and 60%, respectively. The optimal charge and discharge ratios in the presence of two and three DG unit allocation are the same, since the net load on the best bus location and presence of DG units produce minimum power losses. However, the power losses are significantly reduced with the allocation of three DG units and optimal charging and discharging of PEVs. The results of power losses with the optimal allocation of three DG units and optimal coordinated charging are presented in Figure 20.

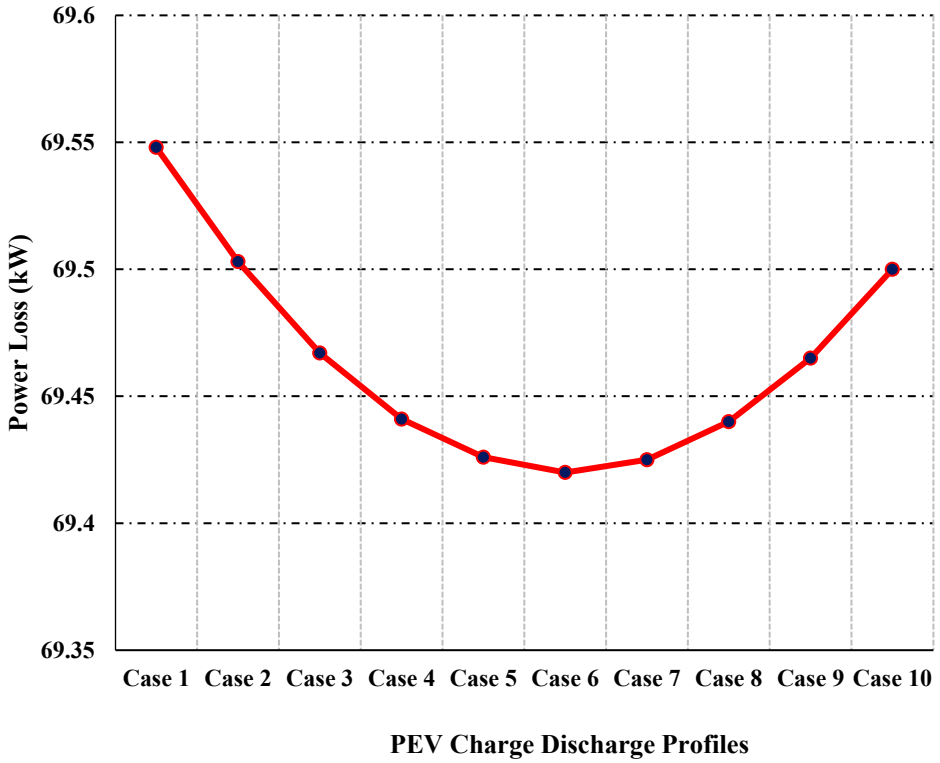

Figure 20. Charge and discharge ratios of PEVs against power loss in presence of 3 DG unit.

4. Conclusions and Future Works

The proposed study develops a deterministic methodology to maximize the accommodation of PEVs and percentage power loss reduction (%PLR). Initially, the PEVs are accommodated on an optimal bus location, which is selected based on the loading capability to power loss index (LCPLI). The accommodation profile is developed based on the uncertainty parameters of PEVs, including battery capacity (BC) and current state of charge (SoC). Then, the DG units are optimally allocated to improve %PLR using the hybrid arithmetic optimization algorithm salp swarm algorithm (AOASSA). In the end, the V2G mode of PEV is adopted to minimize power losses in the presence of fixed PEV load and DG sizes on the best bus location. The results reveal that the best bus is bus-2, since it has highest value of LCPLI in IEEE-33 bus and IEEE-69 bus RDNs. The best bus can accommodate a maximum of 31,988 and 92,519 units of PEVs in IEEE-33 bus and IEEE-69 bus RDNs, respectively. The proposed AOASSA produces at least 0.09% and 0.25% fewer power losses compared with recent contending algorithms applied on IEEE-33 bus and IEEE-69 bus RDNs, respectively. Moreover, the optimal charging and discharging ratios of PEVs further improved the %PLR by 3.08%, 4.19%, and 2.29% in the presence of optimal allocation of one, two and three DG units, respectively in a IEEE-33 bus RDN. On the other hand, the %PLR further improved by 0.09%, 0.09%, and 0.08% with optimal charge and discharge ratios in the presence of one, two and three DG units, respectively, in IEEE-69 bus RDN. Although the proposed study develops a deterministic methodology to maximize PEVs and minimize power losses, a great deal of work can still be extended for future researchers. The researchers can simultaneously maximize PEV accommodation and minimize power losses using multi-objective weighted summation models or Pareto front optimization. Furthermore, an advanced taxonomy of the algorithm can be developed to minimize power losses with optimal allocation of DG units. The proposed study can serve as a benchmark for upcoming research in the subject area.

Author Contributions: Resources, H.M.M. and F.A.; Writing—original draft, Z.A.M.; Writing—review & editing, M.Y.H., D.M.S. and H.M.M.; Supervision, D.M.S. and M.Y.H.; Funding acquisition, F.A. and S.A. All authors have read and agreed to the published version of the manuscript.

Funding: This research received no external funding.

Acknowledgments: This work was supported by the Researchers Supporting Project number (RSPD2023R646), King Saud University, Riyadh, Saudi Arabia. In addition, the authors would also like to acknowledge the Centre of Electrical Energy Systems (CEES), Universiti Teknologi Malaysia (UTM), Malaysia, Mehran University of Engineering & Technology (MUET), Pakistan, and the Higher Education Commission (HEC), Pakistan, for their unlimited support.

Conflicts of Interest: The authors declare no conflict of interest.

References

1. Turkdogan, S. Design and optimization of a solely renewable based hybrid energy system for residential electrical load and fuel cell electric vehicle. *Eng. Sci. Technol. Int. J.* **2021**, *24*, 397–404. [CrossRef]
2. Ari, A.; Arregui, N.; Black, S.; Celasun, O.; Iakova, D.; Mineshima, A.; Mylonas, V.; Parry, I.; Teodoru, I.; Zhunussova, K. Surging energy prices in Europe in the aftermath of the war: How to support the vulnerable and speed up the transition away from fossil fuels. *IMF Work. Pap.* **2022**, *152*, 1–41.
3. Bukar, A.L.; Tan, C.W.; Said, D.M.; Dobi, A.M.; Ayop, R.; Alsharif, A. Energy management strategy and capacity planning of an autonomous microgrid: Performance comparison of metaheuristic optimization searching techniques. *Renew. Energy Focus* **2022**, *40*, 48–66. [CrossRef]
4. Bukar, A.L.; Tan, C.W.; Lau, K.Y.; Toh, C.L.; Ayop, R.; Dahiru, A.T. Energy Management Strategy and Capacity Planning of an Autonomous Microgrid: A Comparative Study of Metaheuristic Optimization Searching Techniques. In Proceedings of the 5th IEEE Conf Energy Conversion, CENCON 2021, Virtual, 25–26 October 2021; pp. 190–195. [CrossRef]
5. Paend, M.; Id, B.; Salam, Z.; Rauf, A.; Id, B.; Ullah, U.; Khan, N.; Anjum, W. Techno-economic modelling of hybrid energy system to overcome the load shedding problem: A case study of Pakistan. *PLoS ONE* **2022**, *17*, e0266660. [CrossRef]
6. Soomro, M.A.; Memon, Z.A.; Kumar, M.; Baloch, M.H. Wind energy integration: Dynamic modeling and control of DFIG based on super twisting fractional order terminal sliding mode controller. *Energy Rep.* **2021**, *7*, 6031–6043. [CrossRef]
7. Khalid, M.; Ahmad, F.; Panigrahi, B.K.; Rahman, H. A capacity efficient power distribution network supported by battery swapping station. *Int. J. Energy Res.* **2022**, *46*, 4879–4894. [CrossRef]
8. Farahmand, M.Z.; Javadi, S.; Sadati, S.M.B.; Laaksonen, H.; Shafie-khah, M. Optimal Operation of Solar Powered Electric Vehicle Parking Lots Considering Different Photovoltaic Technologies. *Clean Technol.* **2021**, *3*, 503–518. [CrossRef]
9. Sultana, U.; Khairuddin, A.; Rasheed, N.; Qazi, S. Allocation of distributed generation and battery switching stations for electric vehicle using whale optimiser algorithm Allocation of distributed generation and battery switching stations for electric vehicle using whale optimiser algorithm. *J. Eng. Res.* **2018**, *6*, 70–93.
10. Rezaei, M.; Moradi, M.H.; Amini, M.H. A simultaneous approach for optimal allocation of renewable energy sources and electric vehicle charging stations in smart grids based on improved GA-PSO algorithm. *Sustain. Cities Soc.* **2017**, *32*, 627–637.
11. Tan, M.; Ates, Y.; Erdinc, O.; Gokalp, E.; Catalão, J.P.S. Effect of electric vehicle parking lots equipped with roof mounted photovoltaic panels on the distribution network. *Electr. Power Energy Syst.* **2019**, *109*, 283–289.
12. Amjad, M.; Ahmad, A.; Ahmed, M.; Hussain, T.U. A review of EVs charging: From the perspective of energy optimization, optimization approaches, and charging techniques. *Transp. Res. Part D* **2018**, *62*, 386–417. [CrossRef]
13. Said, D.; Mouftah, H.T. A Novel Electric Vehicles Charging/Discharging Management Protocol Based on Queuing Model. *IEEE Trans. Intell. Veh.* **2020**, *5*, 100–111. [CrossRef]
14. Gil-González, W.; Garces, A.; Montoya, O.D.; Hernández, J.C. A mixed-integer convex model for the optimal placement and sizing of distributed generators in power distribution networks. *Appl. Sci.* **2021**, *11*, 627. [CrossRef]
15. El-Khattam, W.; Salama, M.M.A. Distributed generation technologies, definitions and benefits. *Electr. Power Syst. Res.* **2004**, *71*, 119–128. [CrossRef]
16. Ackermann, T.; Andersson, G.; Söder, L. Distributed generation: A definition. *Electr. Power Syst. Res.* **2001**, *57*, 195–204. [CrossRef]
17. Pepermans, G.; Driesen, J.; Haeseldonckx, D.; Belmans, R.; D'haeseleer, W. Distributed generation: Definition, benefits and issues. *Energy Policy* **2005**, *33*, 787–798. [CrossRef]
18. Himabindu, N.; Hampannavar, S.; Deepa, B.; Swapna, M. Analysis of microgrid integrated Photovoltaic (PV) Powered Electric Vehicle Charging Stations (EVCS) under different solar irradiation conditions in India: A way towards sustainable development and growth. *Energy Rep.* **2021**, *7*, 8534–8547. [CrossRef]
19. Zeng, B.; Zhu, Z.; Zhu, X.; Qin, L.; Liu, J.; Zhang, M. Estimation of Distribution System Capability for Accommodating Electric Vehicles. *J. Electr. Syst.* **2020**, *16*, 131–141.
20. Said, D. A Survey on Information Communication Technologies in Modern Demand Side Management for Smart Grids: Challenges, Solutions, and Opportunities. *IEEE Eng. Manag. Rev.* **2022**, *51*, 76–107. [CrossRef]

21. Kongjeen, Y.; Bhumkittipich, K.; Mithulananthan, N. Optimal DG sizing and location in modern power grids using PEVs load demand probability. *Trans. Electr. Eng. Electron. Commun.* **2019**, *17*, 51–59. [CrossRef]
22. Tang, H.; Wu, J. Multi-objective coordination optimisation method for DGs and EVs in distribution networks. *Arch. Electr. Eng.* **2019**, *68*, 15–32. [CrossRef]
23. Fazelpour, F.; Vafaeipour, M.; Rahbari, O.; Rosen, M.A. Intelligent optimization of charge allocation for plug-in hybrid electric vehicles utilizing renewable energy considering grid characteristics. In Proceedings of the 2013 IEEE International Conference on Smart Energy Grid Engineering (SEGE), Oshawa, ON, Canada, 28–30 August 2013; pp. 28–30. [CrossRef]
24. Ahmad, F.; Khalid, M.; Panigrahi, B.K. An enhanced approach to optimally place the solar powered electric vehicle charging station in distribution network. *J. Energy Storage* **2021**, *42*, 103090. [CrossRef]
25. Deng, Q.; Feng, C.; Wen, F.; Tseng, C.-L.; Wang, L.; Zou, B.; Zhang, X. Evaluation of Accommodation Capability for Electric Vehicles of a Distribution System Considering Coordinated Charging Strategies. *Energies* **2019**, *12*, 3056. [CrossRef]
26. Chiodo, E.; Fantauzzi, M.; Lauria, D.; Mottola, F. A Probabilistic Approach for the Optimal Sizing of Storage Devices to Increase the Penetration of Plug-in Electric Vehicles in Direct Current Networks. *Energies* **2018**, *11*, 1238. [CrossRef]
27. Amini, M.H.; Parsa, M.; Karabasoglu, O. Simultaneous allocation of electric vehicles' parking lots and distributed renewable resources in smart power distribution networks. *Sustain. Cities Soc.* **2017**, *28*, 332–342. [CrossRef]
28. Shaaban, M.F.; Member, S.; Atwa, Y.M.; Member, S.; El-saadany, E.F.; Member, S. PEVs Modeling and Impacts Mitigation in Distribution Networks. *IEEE Trans. Power Syst.* **2013**, *28*, 1122–1131. [CrossRef]
29. Memon, Z.A.; Hassan, M.Y.; Said, D.M.; Leghari, Z.H.; Shaikh, P.H. A Systematic Approach to Accommodate Plug-in Electric Vehicles in Distribution Networks with Optimal Integration of Distributed Generation. In Proceedings of the 6th International Conference on Electrical, Control and Computer Engineering, Pahang, Malaysia, 23 August 2022; pp. 339–352. [CrossRef]
30. Leemput, N.; Geth, F.; Van Roy, J.; Büscher, J.; Driesen, J. Sustainable Energy, Grids and Networks Reactive power support in residential LV distribution grids through electric vehicle charging. *Sustain. Energy Grids Netw.* **2015**, *3*, 24–35. [CrossRef]
31. Zhao, J.; Wang, J.; Xu, Z.; Wang, C.; Wan, C.; Chen, C. Distribution Network Electric Vehicle Hosting Capacity Maximization: A Chargeable Region Optimization Model. *IEEE Trans. Power Syst.* **2017**, *32*, 4119–4130. [CrossRef]
32. Avila-Rojas, A.E.; De Oliveira-De Jesus, P.M.; Alvarez, M. Distribution network electric vehicle hosting capacity enhancement using an optimal power flow formulation. *Electr. Eng.* **2022**, *104*, 1337–1348. [CrossRef]
33. Zuluaga-Ríos, C.D.; Villa-Jaramillo, A.; Saldarriaga-Zuluaga, S.D. Evaluation of Distributed Generation and Electric Vehicles Hosting Capacity in Islanded DC Grids Considering EV Uncertainty. *Energies* **2022**, *15*, 7646. [CrossRef]
34. Bin Humayd, A.S.; Bhattacharya, K. Assessment of distribution system margins to accommodate the penetration of plug-in electric vehicles. In Proceedings of the 2015 IEEE Transportation Electrification Conference and Expo (ITEC), Dearborn, MI, USA, 14–17 June 2015; pp. 1–6. [CrossRef]
35. Zárate-Miñano, R.; Flores Burgos, A.; Carrión, M. Analysis of different modeling approaches for integration studies of plug-in electric vehicles. *Int. J. Electr. Power Energy Syst.* **2020**, *114*, 105398. [CrossRef]
36. Hazazi, K.M.; Mehmood, K.K.; Cho, G.; Kim, C. Optimal Planning of Distributed Generators for Loss Reduction and Voltage Profile Enhancement Considering the Integration of Electric Vehicles. In Proceedings of the TENCON 2018—2018 IEEE Region 10 Conference, Jeju, Republic of Korea, 28–31 October 2018; pp. 883–888.
37. Moradijoz, M.; Member, S.; Ghazanfarimeymand, A.; Member, S.; Moghaddam, M.P.; Haghifam, M.R. Optimum Placement of Distributed Generation and Parking Lots for Loss Reduction in Distribution Networks. In Proceedings of the 2012 Proceedings of 17th Conference on Electrical Power Distribution, Tehran, Iran, 2–3 May 2012; pp. 1–5.
38. Baharudin, M.A. Minimization of Power Losses in Distribution System via Sequential Placement of Distributed Generation and Charging Station. *Arab. J. Sci. Eng.* **2014**, *39*, 3023–3031. [CrossRef]
39. Moradi, M.H.; Abedini, M.; Tousi, S.M.R.; Hosseinian, S.M. Electrical Power and Energy Systems Optimal siting and sizing of renewable energy sources and charging stations simultaneously based on Differential Evolution algorithm. *Int. J. Electr. Power Energy Syst.* **2015**, *73*, 1015–1024. [CrossRef]
40. Sultana, U.; Khairuddin, A.B.; Sultana, B.; Rasheed, N.; Hussain, S.; Riaz, N. Placement and sizing of multiple distributed generation and battery swapping stations using grasshopper optimizer algorithm. *Energy* **2018**, *165*, 408–421. [CrossRef]
41. Jha, B.K. Coordinated effect of PHEVs with DGs on distribution network. *Int. Trans. Electr. Energy Syst.* **2019**, *29*, e2800. [CrossRef]
42. Kanwar, N.; Gupta, N.; Niazi, K.R.; Swarnkar, A. Optimal distributed generation allocation in radial distribution systems considering customer-wise dedicated feeders and load patterns. *J. Mod. Power Syst. Clean Energy* **2015**, *3*, 475–484. [CrossRef]
43. Anjum, Z.M.; Said, D.M.; Hassan, M.Y.; Leghari, Z.H.; Sahar, G. Parallel operated hybrid Arithmetic-Salp swarm optimizer for optimal allocation of multiple distributed generation units in distribution networks. *PLoS ONE* **2022**, *17*, e0264958. [CrossRef]
44. Abualigah, L.; Diabat, A.; Mirjalili, S.; Abd Elaziz, M.; Gandomi, A.H. The Arithmetic Optimization Algorithm. *Comput. Methods Appl. Mech. Eng.* **2021**, *376*, 113609. [CrossRef]
45. Leghari, Z.H.; Hussain, S.; Memon, A.; Memon, A.H.; Baloch, A.A. Parameter-Free Improved Best-Worst Optimizers and Their Application for Simultaneous Distributed Generation and Shunt Capacitors Allocation in Distribution Networks. *Int. Trans. Electr. Energy Syst.* **2022**, *2022*, 6833488. [CrossRef]
46. Tasnim, S.; Uddin, J.; Tahsin, S.; Anam, K. Developing Efficient Charging Schedule of Electrical Vehicles for Centralized Charging Station by Analyzing Impact on Distribution Network Due to EV Charging. *EJCE Eur. J. Electr. Eng. Comput. Sci.* **2020**, *4*, 1–7. [CrossRef]

47. Leghari, Z.H.; Hassan, M.Y.; Said, D.M.; Jumani, T.A.; Memon, Z.A. A novel grid-oriented dynamic weight parameter based improved variant of Jaya algorithm. *Adv. Eng. Softw.* **2020**, *150*, 102904. [CrossRef]
48. Leghari, Z.H.; Hassan, M.Y.; Said, D.M.; Memon, Z.A.; Hussain, S. An efficient framework for integrating distributed generation and capacitor units for simultaneous grid-connected and islanded network operations. *Int. J. Energy Res.* **2021**, *45*, 14920–14958. [CrossRef]